◀**Fig. 1 Phylogenetic analysis of isolated BtCoVs.** A phylogenetic tree was constructed by the maximum-likelihood method, using a conserved 372-nt sequence from the *RdRp* genes of isolates of BtCoV. Virus lineages detected in this study are marked with black circles. The percentage of replicate trees in which the associated taxa clustered in the bootstrap test (1000 replicates) is shown next to the branches. Phylogenetic analysis was performed using MEGA5 [17]. This model was selected by a modelfit using MEGA5 [17]. Coronaviral sequences used for comparison and their GenBank accession numbers were as follows: human coronavirus 229E (HCoV 229E; NC_002645), human coronavirus NL63 (HCoV NL63; NC_005831), human coronavirus OC43 (NC_005147), human coronavirus HKU1 (NC_006577), SARS coronavirus (NC_004718), canine coronavirus (AF_124986), feline infectious peritonitis virus (FIPV; AY_994055), transmissible gastroenteritis virus (TGEV; NC_002306), porcine epidemic diarrhea virus (PEDV; NC_00 3436), porcine hemagglutinating encephalomyelitis virus (PHEV; NC_007732), bovine coronavirus (NC_003045), murine hepatitis virus (MHV; NC_001846), avian infectious bronchitis virus (IBV; NC_001451), turkey coronavirus isolate MG10 (EU095850), BtCoV HKU2 (DQ249235), BtCoV HKU6 (DQ_249224), BtCoV HKU7 (DQ_249226), BtCoV HKU8 (NC_010438), BtCoV HKU9-1 (EF_065513), BtCoV HKU9-3 (EF_065515), bat SARS-CoV Rf1 (DQ_412042), BtCoV/A970/2005 (DQ_648854), BtCoV/A515/2005 (DQ_648822), BtKY22/Chaerephon sp./Kenya/2006 (HQ728486), BtCoV/Philippines/Dilliman1552G1/2008 (AB_539080) and BtCoV/Philippines/Dilliman/1525G2/2008 (AB_539081)

protein was confirmed by CBB staining and WB using an anti-6x His antibody (Fig. 2). As the recombinant N protein was present in the pellet after centrifugation, this pellet was resuspended in phosphate-buffered saline (PBS) containing 0.5 % Triton X-100. It was confirmed that the recombinant protein was pure and showed a single band in WB using an anti-6x His antibody (Fig. 2b). The secondary supernatant (isolated after two rounds of centrifugation of the *E. coli* cells) was used as antigen to detect antibodies to BtCoV. Bat serum samples that detected a 63-kDa band at a dilution of 1:1000 were considered positive (Fig. 2c). Sera from 10 Leschnault rousette bats (*Rousettus leschnaulti*), which were obtained from a zoo in Japan, were used as negative controls; none showed bands at 63 kDa. As a positive control, serum from coronavirus infected Leschnault rousette bat was used [14]. Table 1 displays the prevalence of anti-BtCoV antibodies; 119/179 (66.5 %) serum specimens had antibody against N protein. Total WB positivity correlated with total RT-PCR positivity ($p < 0.01$, Fisher's exact test).

Our surveys revealed that diverse populations of BtCoVs are continuously circulating in bats in the Philippines. Interestingly, CoVs in two different lineages were detected in greater musky fruit bats (BtCoV/Philippines/Diliman1525G2/2008 and BtCoV2265/Philippines/2010). Because this bat species is endemic to the Philippines [18], BtCoVs may have adapted to the local bat species and developed a unique ecology. While the bat-CoV/Philippines/Diliman1525G2/2008 lineage was only present in

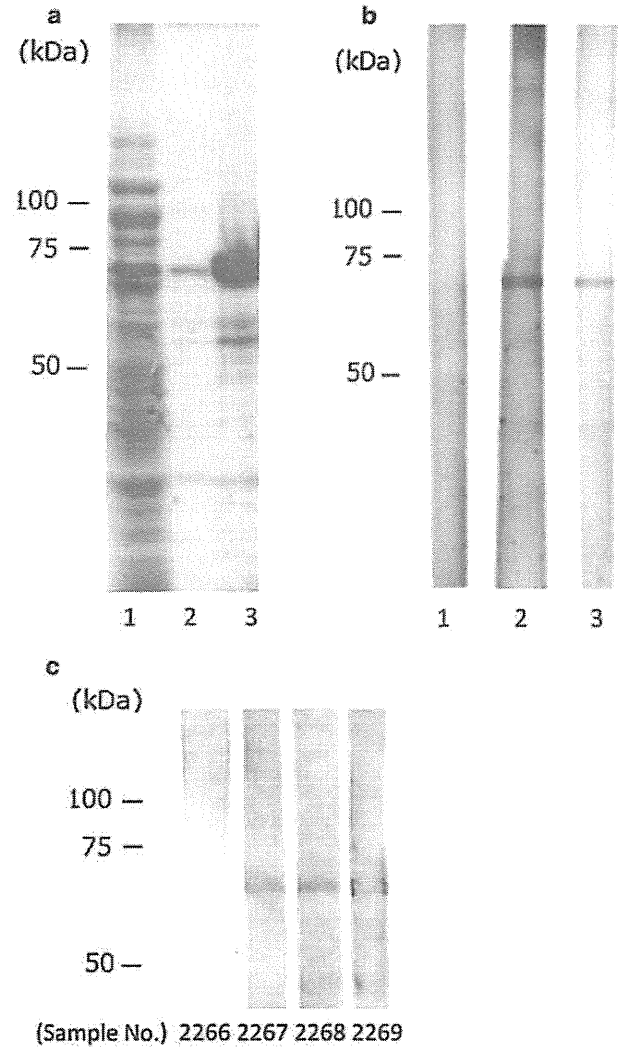

Fig. 2 Expression and western blotting of the recombinant BtCoV N protein. (a) CBB staining of the recombinant N protein. BL21 (DE3) cells expressing recombinant N protein were suspended in PBS containing 1 % Triton X-100, followed by sonication and centrifugation. Supernatants were collected (lane 1), and the pellet was resuspended in 0.5 % Triton X-100/PBS. After another round of centrifugation, the secondary supernatant was collected (lane 2). Two supernatant samples and the pellet (lane 3) were analyzed by SDS-PAGE. The gel was stained with CBB. (b) Western blotting of the recombinant N protein. Secondary supernatant (lane 2 in a) was separated by 8 % SDS-PAGE and detected by serum from a CoV-negative bat (lane 1 diluted 1:1000), serum from a BtCoV-infected bat (lane 2, diluted 1:1000) [14], and HRP-conjugated anti-6x His antibody (lane 3, diluted 1:5000). Strips incubated with bat sera were subsequently detected using rabbit anti-bat IgG antibody (diluted 1:1000) as the secondary antibody, and HRP-conjugated anti-rabbit IgG antibody (diluted 1:2000) as the tertiary antibody. (c) WB analysis of bat sera. Recombinant BtCoV N protein was detected by bat serum specimens as described in Fig. 2b

lesser dog-faced fruit bats and greater musky fruit bats, the BtCoV2265/Philippines/2010 lineage was detected in various bat species, including both insectivorous and

frugivorous bats. These observations imply that interspecies jumping has occurred with BtCoVs in the Philippines. Given the wide host range of mammalian coronaviruses, it would not be surprising if BtCoVs crossed species barriers between frugivorous and insectivorous bats as well as barriers between different frugivorous bats. Besides SARS-CoV, cross-species transmission events have been implicated in the emergence of novel CoVs [19]. Recombination commonly occurs among CoVs [20] and also seems to happen in BtCoVs [21]. These two features could enable novel BtCoVs to emerge, leading to diversity and complexity among BtCoVs.

While numerous surveys to detect BtCoV RNA have been conducted, serological studies to find anti-CoV antibodies in bats are limited. It is possible that this lack of information has made our understanding of BtCoVs obscure. Only a few studies have investigated antibodies to SARS-related coronavirus in bats [4, 22, 23]. Our survey revealed that antibodies to BtCoV N protein were highly prevalent in bat species (66.5 %). This observation also supports the idea of continuous circulation of BtCoVs in the Philippines and implies that repetitive infection enables BtCoVs to circulate among bat colonies.

We previously reported two lineages of BtCoVs in the Philippines. One was an alphacoronavirus and the other was a betacoronavirus. In this study, we found two more distinct lineages: a betacoronavirus related to another previously described virus [14] and a novel alphacoronavirus. Our genetic and serological surveys suggest the widespread distribution and diversity of BtCoVs in the Philippines.

Acknowledgments We greatly thank Mr. Edison Cosico and Mr. Eduardo Eres for the arrangements for bat collection. This study was supported by a grant from a Ministry of Education, Culture, Sports, Science and Technology, Japan.

References

1. Cc H, Hk V, Ds R, Tony S, Paul C (2008) Bats prove to be rich reservoirs for emerging viruses. Microbe 3:521–528
2. Drosten C, Günther S, Preiser W, van der Werf S, Brodt HR, Becker S, Rabenau H, Panning M, Kolesnikova L, Fouchier RA, Berger A, Burguière AM, Cinatl J, Eickmann M, Escriou N, Grywna K, Kramme S, Manuguerra JC, Müller S, Rickerts V, Stürmer M, Vieth S, Klenk HD, Osterhaus AD, Schmitz H, Doerr HW (2003) Identification of a novel coronavirus in patients with severe acute respiratory syndrome. N Engl J Med 348:1967–1976
3. WHO (2003) Cumulative number of reported probable cases of Severe Acute Respiratory Syndrome (SARS). http://www.who.int/csr/sars/country/2003_05_20/en/. Accessed 27 November 2011
4. Lau SK, Woo PC, Li KS, Huang Y, Tsoi HW, Wong BH, Wong SS, Leung SY, Chan KH, Yuen KY (2005) Severe acute respiratory syndrome coronavirus-like virus in Chinese horseshoe bats. Proc Natl Acad Sci USA 102:14040–14045
5. Li W, Shi Z, Yu M, Ren W, Smith C, Epstein JH, Wang H, Crameri G, Hu Z, Zhang H, Zhang J, McEachern J, Field H, Daszak P, Eaton BT, Zhang S, Wang LF (2005) Bats are natural reservoirs of SARS-like coronaviruses. Science 310:676–679
6. Tong S, Conrardy C, Ruone S, Kuzmin IV, Guo X, Tao Y, Niezgoda M, Haynes L, Agwanda B, Breiman RF, Anderson LJ, Rupprecht CE (2009) Detection of novel SARS-like and other coronaviruses in bats from Kenya. Emerg Infect Dis 15:482–485
7. Carrington CV, Foster JE, Zhu HC, Zhang JX, Smith GJ, Thompson N, Auguste AJ, Ramkissoon V, Adesiyun AA, Guan Y (2008) Detection and phylogenetic analysis of group 1 coronaviruses in South American bats. Emerg Infect Dis 14:1890–1893
8. Gloza-Rausch F, Ipsen A, Seebens A, Göttsche M, Panning M, Felix Drexler J, Petersen N, Annan A, Grywna K, Müller M, Pfefferle S, Drosten C (2008) Detection and prevalence patterns of group I coronaviruses in bats, northern Germany. Emerg Infect Dis 14:626–631
9. Dominguez SR, O'Shea TJ, Oko LM, Holmes KV (2007) Detection of group 1 coronaviruses in bats in North America. Emerg Infect Dis 13:1295–1300
10. Poon LL, Chu DK, Chan KH, Wong OK, Ellis TM, Leung YH, Lau SK, Woo PC, Suen KY, Yuen KY, Guan Y, Peiris JS (2005) Identification of a novel coronavirus in bats. J Virol 79:2001–2009
11. Donaldson EF, Haskew AN, Gates JE, Huynh J, Moore CJ, Frieman MB (2010) Metagenomic analysis of the viromes of three North American bat species: viral diversity among different bat species that share a common habitat. J Virol 84:13004–13018
12. Li L, Victoria JG, Wang C, Jones M, Fellers GM, Kunz TH, Delwart E (2010) Bat guano virome: predominance of dietary viruses from insects and plants plus novel mammalian viruses. J Virol 84:6955–6965
13. Vijaykrishna D, Smith GJ, Zhang JX, Peiris JS, Chen H, Guan Y (2007) Evolutionary insights into the ecology of coronaviruses. J Virol 81:4012–4020
14. Watanabe S, Masangkay JS, Nagata N, Morikawa S, Mizutani T, Fukushi S, Alviola P, Omatsu T, Ueda N, Iha K, Taniguchi S, Fujii H, Tsuda S, Endoh M, Kato K, Tohya Y, Kyuwa S, Yoshikawa Y, Akashi H (2010) Bat coronaviruses and experimental infection of bats, the Philippines. Emerg Infect Dis 16:1217–1223
15. Omatsu T, Ishii Y, Kyuwa S, Milanda EG, Terao K, Yoshikawa Y (2003) Molecular evolution inferred from immunological cross-reactivity of immunoglobulin G among Chiroptera and closely related species. Exp Anim 52:425–428
16. Tang XC, Zhang JX, Zhang SY, Wang P, Fan XH, Li LF, Li G, Dong BQ, Liu W, Cheung CL, Xu KM, Song WJ, Vijaykrishna D, Poon LL, Peiris JS, Smith GJ, Chen H, Guan Y (2006) Prevalence and genetic diversity of coronaviruses in bats from China. J Virol 80:7481–7490
17. Tamura K, Peterson D, Peterson N, Stecher G, Nei M, Kumar S (2011) MEGA5: molecular evolutionary genetics analysis using maximum likelihood, evolutionary distance, and maximum parsimony methods. Mol Biol Evol 28:2731–2739
18. Ong P, Rosell-Ambal G, Tabaranza B, Heaney L, Pedregosa M, Paguntalan LM, Cariño AB, Ramayla S, Duya P, Warguez D, Alcala E, Garcia H, Pamaong R, Gonzalez JC, Lorica RP (2008) IUCN RedList of Thresatened Species. http://www.iucn.org. Accessed 1 February 2012
19. Vijgen L, Keyaerts E, Moës E, Thoelen I, Wollants E, Lemey P, Vandamme AM, Van Ranst M (2005) Complete genomic sequence of human coronavirus OC43: molecular clock analysis suggests a relatively recent zoonotic coronavirus transmission event. J Virol 79:1595–1604
20. Masters PS (2006) The molecular biology of coronaviruses. Adv Virus Res 66:193–292

21. Lau SK, Li KS, Huang Y, Shek CT, Tse H, Wang M, Choi GK, Xu H, Lam CS, Guo R, Chan KH, Zheng BJ, Woo PC, Yuen KY (2010) Ecoepidemiology and complete genome comparison of different strains of severe acute respiratory syndrome-related Rhinolophus bat coronavirus in China reveal bats as a reservoir for acute, self-limiting infection that allows recombination events. J Virol 84:2808–2819
22. Müller MA, Paweska JT, Leman PA, Drosten C, Grywna K, Kemp A, Braack L, Sonnenberg K, Niedrig M, Swanepoel R (2007) Coronavirus antibodies in African bat species. Emerg Infect Dis 13:1367–1370
23. Lau SKP, Poon RWS, Wong BHL, Wang M, Huang Y, Xu H, Guo R, Li KSM, Gao K, Chan K-H, Zheng B-J, Woo PCY, Yuen K-Y (2010) Coexistence of different Genotypes in the same bat and sCharacterization of rousettus bat coronavirus HKU9 belonging to a novel betacoronavirus subgroup. J Virol 84:11385–11394

BioOne RESEARCH EVOLVED

Efficacy of Soluble Recombinant FliC Protein from *Salmonella enterica* Serovar Enteritidis as a Potential Vaccine Candidate Against Homologous Challenge in Chickens

Author(s): Masashi Okamura, Wakako Matsumoto, Fumio Seike, Yuuya Tanaka, Chie Teratani, Maki Tozuka, Takashige Kashimoto, Kazuaki Takehara, Masayuki Nakamura and Yasuhiro Yoshikawa
Source: Avian Diseases, 56(2):354-358. 2012.
Published By: American Association of Avian Pathologists
DOI: http://dx.doi.org/10.1637/9986-111011-Reg.1
URL: http://www.bioone.org/doi/full/10.1637/9986-111011-Reg.1

BioOne (www.bioone.org) is a nonprofit, online aggregation of core research in the biological, ecological, and environmental sciences. BioOne provides a sustainable online platform for over 170 journals and books published by nonprofit societies, associations, museums, institutions, and presses.

Your use of this PDF, the BioOne Web site, and all posted and associated content indicates your acceptance of BioOne's Terms of Use, available at www.bioone.org/page/terms_of_use.

Usage of BioOne content is strictly limited to personal, educational, and non-commercial use. Commercial inquiries or rights and permissions requests should be directed to the individual publisher as copyright holder.

BioOne sees sustainable scholarly publishing as an inherently collaborative enterprise connecting authors, nonprofit publishers, academic institutions, research libraries, and research funders in the common goal of maximizing access to critical research.

AVIAN DISEASES 56:354–358, 2012

Efficacy of Soluble Recombinant FliC Protein from *Salmonella enterica* Serovar Enteritidis as a Potential Vaccine Candidate Against Homologous Challenge in Chickens

Masashi Okamura,[AE] Wakako Matsumoto,[A] Fumio Seike,[A] Yuuya Tanaka,[A] Chie Teratani,[A] Maki Tozuka,[A] Takashige Kashimoto,[B] Kazuaki Takehara,[AC] Masayuki Nakamura,[AD] and Yasuhiro Yoshikawa[A]

[A]Laboratory of Zoonoses, Kitasato University School of Veterinary Medicine, Towada, Aomori 034-8628, Japan
[B]Laboratory of Veterinary Public Health, Kitasato University School of Veterinary Medicine, Towada, Aomori 034-8628, Japan

Received 16 November 2011; Accepted 6 January 2012; Published ahead of print 9 January 2012

SUMMARY. FliC, the flagellin antigen of *Salmonella* Enteritidis, was tested as a vaccine candidate for protective effect against a homologous challenge in chickens. After immunization with recombinant FliC (rFliC) or administration of phosphate-buffered saline (PBS) at 56 days old, the chickens were challenged with 10^9 colony-forming units of *Salmonella* Enteritidis at 76 days old. The vaccinated birds showed significantly decreased bacterial counts in the liver and cecal contents compared to those administered PBS at 7 days postchallenge, but the protection was partial. The replication experiment also showed a similar result. In both experiments, vaccination induced an increased level of serum anti-rFliC IgG, which was also reactive to the native flagella. The intestinal IgA level was slightly higher in the vaccinated birds than in the control. However, neither the proliferative response nor interferon-γ secretion of splenic cells upon stimulation with rFliC was induced. Therefore, the effect of rFliC as a vaccine is limited, and further improvement is needed.

RESUMEN. Eficacia de la proteína recombinante soluble FliC de *Salmonella enterica* serovar Enteritidis como un candidato potencial para una vacuna contra el desafío homólogo en pollos.

El antígeno de flagelina FliC de *Salmonella* Enteritidis, se puso a prueba como un candidato para vacuna en su efecto protector frente a un desafío homólogo en pollos. Después de la inmunización con FliC recombinante (rFliC) o la administración de solución amoriguada de fosfatos (PBS) a los 56 días de edad, los pollos fueron desafiados con 10^9 unidades formadoras de colonias de *Salmonella* Enteritidis a los 76 días de edad. Las aves vacunadas mostraron una disminución significativa de los conteos bacterianos en el hígado y en los contenidos cecales en comparación con las aves a las que se les administró PBS a los siete días después del desafío, pero la protección fue parcial. El experimento de replicación también mostró un resultado similar. En ambos experimentos, la vacunación indujo un aumento de IgG anti-rFliC en el suero, que era también reactiva a los flagelos nativos. El nivel de IgA intestinal fue ligeramente mayor en las aves vacunadas en comparación con las aves del grupo control. Sin embargo, ni la respuesta proliferativa, ni la secreción de γ-interferón por las células del bazo en respuesta a la estimulación con rFliC fue inducida. Por lo tanto, el efecto de la proteína rFliC como una vacuna es limitada, y se requiere de un perfeccionamiento posterior.

Key words: *Salmonella enterica* serovar Enteritidis, flagellin, vaccine

Abbreviations: BSA = bovine serum albumin; CFU = colony-forming units; DHL-rif plate(s) = desoxycholate-hydrogen sulfate-lactose agar plate(s) supplemented with 100 μg/ml of rifampicin; HIB = heart infusion broth; IFN = interferon; IL = interleukin; IPTG = isopropyl β-D-1-thiogalactopyranoside; LPS = lipopolysaccharide; OD = optical density; PBS = phosphate-buffered saline; PBST = phosphate-buffered saline with Tween 20; PCR = polymerase chain reaction; rFliC = recombinant FliC; SE = *Salmonella* Enteritis; SI = stimulation index

Salmonella enterica has been recognized as a major cause of food-borne illness in humans worldwide. The incidence of *Salmonella* infection has increased substantially for decades, with increased cases of *Salmonella enterica* serovar Enteritidis (*Salmonella* Enteritidis) infection due to the consumption of contaminated hen eggs (10). Although a decreased incidence has been reported recently (6,17), major outbreaks still occur in the United Kingdom (13) and the United States (11), causing it to remain relevant to public health. Poultry is the most important source of food-borne salmonellosis in humans; therefore, it is the primary target for the control of *Salmonella* at the production stage of the food chain. Vaccination of poultry is one promising strategy to mitigate *Salmonella* infection in poultry and, in turn, humans as well. Live and killed *Salmonella* vaccines for poultry have been available worldwide. Because potential reversal to virulence through horizontal gene transfer remains a concern for live attenuated vaccines (2), only killed vaccines for laying hens and breeder flocks are available in Japan. However, killed vaccines generally contain not only effective immunogenic antigens but also minor antigens, and may retain potentially adverse components, such as bacterial lipopolysaccharide (LPS) (1). Given the accumulation of LPS, multivalent preparations from whole-cell bacterins of a number of different serovars cannot be reasonable. Therefore, the development of different types of vaccines, such as a component vaccine that consists of only effective antigens with no or a minimal amount of LPS and would be more suitable for multivalent preparations than would whole-cell bacterins, has great value.

Flagella have been considered to be effective antigens to stimulate immune responses because they are exposed to the bacterial surface and easily recognized by the host immune system. Among the flagellar antigens, the FliC protein is assembled into the filament and

[C]Present address: Laboratory of Veterinary Hygiene, Tokyo University of Agriculture and Technology, Fuchu, Tokyo 183-8538, Japan.
[D]Present address: Research Institute for Animal Science in Biochemistry & Toxicology, 3-7-11 Hashimotodai, Midori-ku, Sagamihara, Kanagawa 252-0132, Japan.
[E]Corresponding author. E-mail: okamuram@vmas.kitasato-u.ac.jp

has been considered to contribute not only to motility but also pathogenicity and host innate recognition (5,24). The present study is an evaluation of the efficacy of the FliC as a prototype component vaccine against *Salmonella* in poultry based on the concept that FliC contains the serovar-specific g, m antigenic region and can be used for a potential multivalent vaccine in combination with FliC from different *Salmonella* serovars or other immunogenic antigens in the future.

MATERIALS AND METHODS

Bacteria and growth conditions. *Salmonella* Enteritidis phage type 4 strain HY-1 was made resistant to rifampicin through selective pressure for ease of recovery and used in this study (21). To prepare the bacterial suspension and inocula, the organisms were grown on a desoxycholate-hydrogen sulfate-lactose agar plate supplemented with 100 μg/ml of rifampicin (DHL-rif plate), and one or two isolated colonies were transferred to a heart infusion broth (HIB; Eiken Chemical, Tokyo, Japan) and incubated at 37 C for 5–6 hr with shaking until a density of 10^9 colony-forming units (CFU)/ml was obtained, as determined by optical density at 600 nm (OD_{600}). The bacterial concentration was adjusted by serial dilution with PBS, and the actual inoculation dose was determined retrospectively by colony counts of serial 10-fold dilutions that were spread on DHL-rif plates.

Cloning and expression of *fliC*. The bacterial genomic DNA was extracted with the use of the Qiagen DNeasy Blood & Tissue Kit (Qiagen, Duesseldorf, Germany) according to the manufacturer's instructions. The DNA sequence of the *Salmonella* Enteritidis *fliC* (NCBI Reference Sequence: AY649709.1) was obtained by polymerase chain reaction (PCR) with the use of an Expand High-Fidelity^{PLUS} PCR System (Roche Applied Science, Mannheim, Germany). The *fliC* DNA was amplified with the primer pair of FliC-F (5′-CATATGGCACAAGTCATTAA-TACA-3′) and FliC-R (5′-CTCGAGACGCAGTAAAGAGAGGA-3′); the product lacked the start and stop codons of full-length FliC and instead contained the recognition sites of the restriction enzymes *Nde*I and *Xho*I, respectively (underlined). This allowed the directional cloning of the PCR fragment into the expression vector. The PCR product was cloned into the pGEM-T Easy Vector (Promega, Madison, WI), and the plasmid was transformed into One Shot TOP10 competent *Escherichia coli* (Invitrogen, Carlsbad, CA). The transformed cells were recovered by blue–white selection. The plasmid DNA from the selected clones was sequenced. Digestion of the pGEM-T Easy plasmid with *Nde*I and *Xho*I resulted in restriction fragments of *fliC*, which was subcloned into the expression vector pET29b (Novagen, Milwaukee, WI). This inducible vector system allows the expression of recombinant proteins with a six histidine tag at the *C*-terminus under the presence of isopropyl β-D-1-thiogalactopyranoside (IPTG). The plasmid was transformed into *E. coli* BL21 (DE3) competent cells and grown on LB agar containing 100 μg/ml kanamycin. The recombinant FliC (rFliC) protein was expressed in the soluble fraction under the presence of IPTG and purified under native conditions by affinity chromatography on a Ni-NTA His-Bind Resin (Takara Bio Inc., Shiga, Japan). The purified protein was pooled and dialyzed in Spectra/Por 4 Regenerated Cellulose Dialysis Membranes (Spectrum Laboratories, Inc., Rancho Dominguez, CA). The protein concentration was determined by the DC Protein Assay (Bio-Rad) based on the Lowry method (14). The purified proteins were confirmed to be rFliC by western blotting with the use of antipolyhistidine mouse monoclonal antibody (Sigma, St. Louis, MO) followed by horseradish peroxidase-conjugated anti-mouse IgG rabbit sera (BD Transduction Laboratories, Lexington, KY). Reaction was visualized by the peroxidase substrate (Sigma). On the other hand, crude flagellin was separated according to Okamura *et al.* (18) and used as the native antigen.

Preparation of component vaccine. The concentration of rFliC was adjusted to 370 μg/ml with PBS, and the volume was mixed well with the same volume of complete Freund adjuvant. The vaccination dose was 100 μg in 0.4 ml/bird.

Experimental animals. In the present study, 46-day-old chicks of white leghorn laying hens (Lohman, Julia), none of which had been vaccinated against *Salmonella*, were obtained from a local commercial layer farm. The birds were reared in individual wire cages with a nonmedicated layer ration and water supplied *ad libitum* in an isolation building. The birds were confirmed to be *Salmonella* free by examining fresh cecal droppings as described below. All of the animal experiments in this study followed the institutional guidelines for the care and use of laboratory animals and were approved by the Animal Research Committee, Kitasato University School of Veterinary Medicine, Japan.

Efficacy of vaccination with rFliC. Thirty healthy 46-day-old chicks were divided into two groups, administered intramuscularly with either adjuvant-mixed rFliC or PBS (n = 15/group) in their legs. Immunization was performed at 56 days of age. The spleen and intestinal mucus were collected from five hens of each group at 19 days postimmunization for immunological assays. The remaining hens were challenged orally with 10^9 CFU of *Salmonella* Enteritidis at 20 days postimmunization and five hens of each group were necropsied at 7 and 14 days postchallenge. The liver, spleen, and cecal contents were examined for *Salmonella*. Sera were also collected at 0, 6, 13, 19, 27, and 34 days postimmunization for antibody measurement. The replication experiment was also performed in a similar manner: Immunization at 46 days of age, collection of the spleen and intestinal mucus at 21 days postimmunization, challenge at 22 days postimmunization, necropsy at 6 and 13 days postchallenge, and collection of sera weekly postimmunization.

Recovery of bacteria from cecal droppings and tissue samples. The cecal droppings after challenge and the liver, spleen, and cecal contents at necropsies were taken aseptically and used for enumeration of *Salmonella* according to the previous study (20,21). Briefly, the samples were homogenized with a ninefold volume of Hajna tetrathionate broth (Eiken, Tokyo) for the cecal contents and HIB for the liver and spleen. Serial tenfold dilutions from the homogenates were then spread on DHL-rif plates, and colony counts (detection limit of 400 CFU/g) were recorded after incubation at 37 C for 24 hr (the direct cultures). The homogenates that had been negative for *Salmonella* in the direct culture were also enriched in two phases. The positive samples detected at the primary and secondary enrichment phases were estimated as 100 and 10 CFU/g, respectively.

Measurement of antibody levels in sera and intestinal mucus. Serum IgG and intestinal IgA antibodies against FliC were measured by the enzyme-linked immunosorbent assay according to previous studies (21,23). For both assays, each well of 96-well microtiter plates (Sumitomo Bakelite Co., Ltd., Tokyo, Japan) was coated overnight at 4 C with 50 μl of 10 μg/ml rFliC in a carbonate-bicarbonate buffer. Sera were diluted 10-fold with 0.5% bovine serum albumin-phosphate-buffered saline with Tween 20 (BSA-PBST) applied to the plates at 50 μl/well. For intestinal IgA, mucus from the intestinal lumen was collected in Hanks' balanced salt solution (Sigma) containing 10 mM phenylmethanesulfonylfluoride, 0.01% sodium azide, and 1% BSA and mixed well. After centrifugation at 5000 × g for 30 min at 4 C, supernatants were 10-fold diluted in BSA–PBST and used instead of sera. Rabbit anti-chicken IgG antibody conjugated with horseradish peroxidase (Sigma) or goat anti-chicken IgA antibody conjugated with horseradish peroxidase (Bethyl Laboratories, Montgomery, TX), a peroxidase substrate (Sigma), and 2N H_2SO_4 (50 μl/well) was used for the reaction, and the OD_{450} values were measured. Each assay was performed in duplicate.

Reactivity of vaccine-induced antibody to native flagella and rFliC. Sera collected at 19 days postimmunization (1 day before challenge) and 7 days postchallenge were used for western blot analysis to confirm the reactivity to native flagella and rFliC. Native flagella and rFliC were applied to SDS-PAGE and blotted onto a nitrocellulose membrane Hybond C Extra (GE Healthcare, UK Ltd., Buckinghamshire, United Kingdom). The sera and the rabbit anti-chicken IgG antibody conjugated with horseradish peroxidase (Sigma) diluted at 1:1000 were used and the reaction was visualized by the peroxidase substrate (Sigma).

Splenic cell proliferation assay and measurement of interferon (IFN)-γ. The splenic cells were isolated and used for a cell proliferation assay according to Okamura *et al.* (18). The splenic cells were seeded

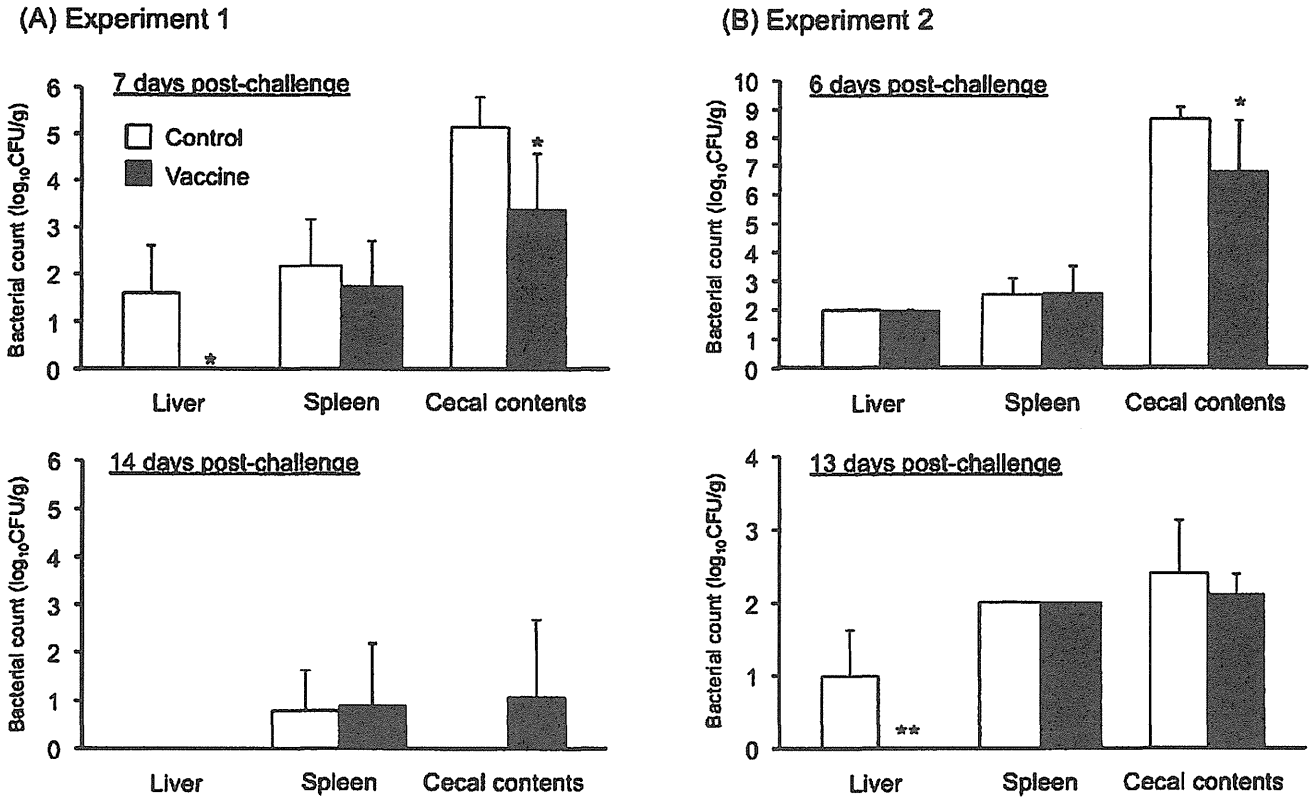

Fig. 1. Bacterial counts from liver, spleen, and cecal contents after challenge in Experiments 1 (A) and 2 (B). n = 5 birds/group. Asterisks indicate significant differences between groups ($P < 0.01$).

into 96-well tissue culture plates at 1.25×10^6 cells/well and stimulated with rFliC (20 μg/ml), concanavalin A (12.5 mg/ml, Sigma) as positive control, or PBS as negative control for 48 hr at 41.5 C and 5% CO_2. Cell proliferation was then determined at OD_{450} with the use of a cell-counting kit (Dojindo Molecular Technologies, Inc., Kumamoto, Japan). Each sample was analyzed in duplicate, and the stimulation index (SI) was calculated with the use of the following formula: SI = mean OD of mitogen- or antigen-stimulated proliferation/mean OD of nonstimulated proliferation. Furthermore, supernatants from the rFliC-stimulated cells were collected, filtered through a 0.45-μm membrane, and used for the measurement of IFN-γ with the use of Chicken IFN-γ Cytoset (Biosource International, Inc., Camarillo, CA) according to the manufacturer's instructions.

Statistical analyses. Data of CFU enumeration, antibody levels, IFN-γ levels, and SI values for splenic cell proliferation were compared between vaccinated and unvaccinated chickens by the unpaired Student t-test. P values of less than 0.05 were considered significant.

RESULTS

In the first experiment, the vaccinated birds showed significantly ($P < 0.01$) decreased bacterial counts in the liver and cecal contents ($<10^2$ CFU/g) compared to those administered PBS at 7 days postchallenge (Fig. 1A). The replication experiment also showed significantly decreased levels of bacteria in the cecal contents at 6 days postchallenge ($P < 0.05$) and in the liver at 13 days postchallenge ($P < 0.01$; Fig. 1B).

On the other hand, vaccination with rFliC successfully induced an increased level of serum anti-FliC IgG in both experiments (the representative data shown in Fig. 2A). A vaccine-induced antibody was reactive not only to rFliC, but also to the native flagella (Fig. 2B). The intestinal IgA level was slightly higher in the vaccinated birds than in the control ones (Fig. 2C). However, neither the proliferative response (Fig. 3A) nor IFN-γ secretion (Fig. 3B) of splenic cells upon stimulation with rFliC was induced.

DISCUSSION

We have previously reported that immunization with *Salmonella* Enteritidis bacterin induces specific cell proliferation, high level production of nitric oxide, increased number of TCRγδ$^+$ cells, and production of IFN-γ and interleukin (IL) -2 in splenic cells upon *ex vivo* stimulation with flagella and IL-1, -2, -6, and -8 and IFN-γ production *in vivo* (18,19). In these studies, a challenge trial could not be performed; thus, we were encouraged to evaluate the potential of flagella as an effective vaccine against *Salmonella* Enteritidis infection in poultry. Another study showed that immunization with SEp9, which was the g, m antigenic region of FliC for *Salmonella* Enteritidis, more effectively reduced the bacterial counts in the cecal contents even at 3 wk postchallenge (25). In this regard, the vaccine efficacy of rFliC in the present study is limited. The inconsistency between these results might be due to differences in the bacterial strains, chicken lines, and/or other factors, such as experimental design. rFliC consists of the g, m antigen and the other regions, which was not included in SEp9 and might also potentially affect our result. On the other hand, the inconsistency in the bacterial counts from the tissue samples and cecal contents at necropsies between trials in the current study might be a consequence of the small number of challenged birds evaluated.

The limited success of rFliC vaccine might be due to the insufficient induction of the host cellular immune responses as

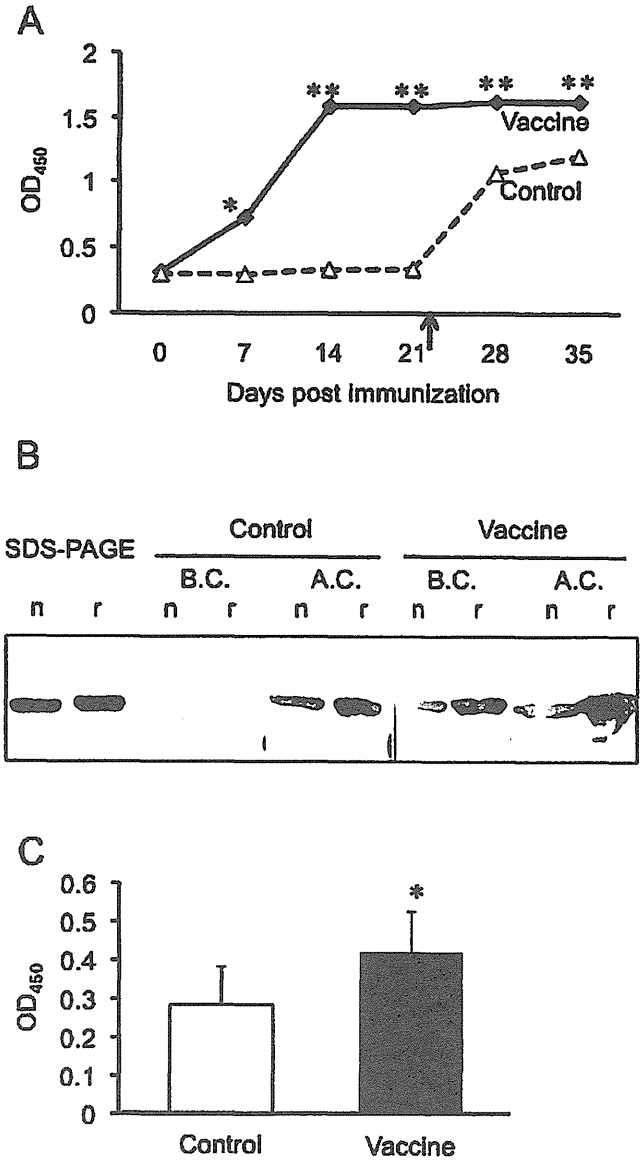

Fig. 2. Antibody responses by rFliC vaccine in the second experiment. (A) Anti-FliC serum IgG response induced by vaccination. n = 15 birds/group (7, 14, and 21 days postimmunization), 10 birds/group (28 days postimmunization), or 5 birds/group (35 days postimmunization). Arrow indicates the date of challenge (22 days postimmunization). (B) Reactivity of vaccine-induced antibody to rFliC and native flagella. B.C., before challenge; A.C., after challenge; n: native flagella; r: rFliC. (C) Anti-rFliC IgA in the intestinal mucus induced by vaccination. Samples were taken just before challenge. Asterisks indicate significant differences between groups ($^*P < 0.05$, $^{**}P < 0.01$).

evidenced by low proliferation and IFN-γ production by stimulated splenic cells. To maximize such responses, the use of novel adjuvants (7) or an effective liposome (8,12), combination with heterologous immunopotent proteins, such as tetanus toxoid (4,22), and/or improvement to the DNA vaccine platform (15) should be considered in the future. In addition, because flagellin has been found to have the good adjuvant activity (16), combination with other immunogenic antigens from homologous bacteria, such as porins (9), can also be the promising approach. More recently, Bobat

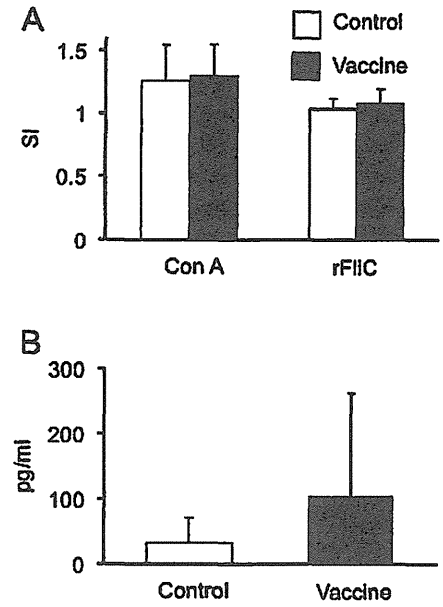

Fig. 3. Cellular responses by rFliC vaccine in the second experiment. (A) Proliferative response of splenic cells upon *ex vivo* stimulation with concanavalin A (Con A) or rFliC. Splenic cells were collected from control and vaccinated birds at 21 days postimmunization. n = 5 birds/group. SI means the stimulation index, which is calculated with the use of the following formula: SI = mean OD of mitogen- or antigen-stimulated proliferation/mean OD of nonstimulated proliferation. (B) Concentration of IFN-γ in the supernatants from the rFliC-stimulated cells. n = five birds/group.

et al. (3) showed that, in mice, some subunit vaccines such as one using soluble recombinant FliC may induce Th2 responses during primary immunization but can develop the protective Th1 immunity during subsequent infection with *Salmonella enterica* serovar Typhimurium. We should evaluate the necessity of designing Th1-inducing vaccines for *Salmonella* control also in poultry.

REFERENCES

1. Arnon, R., M. Shapira, and C. O. Jacob. Synthetic vaccines. J. Immunol. Methods 61:261–273. 1983.

2. Barrow, P. A. Experimental infection of chickens with *Salmonella* enteritidis. Avian Pathol. 120:145–153. 1991.

3. Bobat, S., A. Flores-Langarica, J. Hitchcock, J. L. Marshall, R. A. Kingsley, M. Goodall, C. Gil-Cruz, K. Serre, D. L. Leyton, S. E. Letran, F. Gaspal, R. Chester, J. L. Chamberlain, G. Dougan, C. Lopez-Macias, I. R. Henderson, J. Alexander, I. C. MacLennan, and A. F. Cunningham. Soluble flagellin, FliC, induces an Ag-specific Th2 response, yet promotes T-bet-regulated Th1 clearance of *Salmonella* typhimurium infection. Eur. J. Immunol. 41:1606–1618. 2011.

4. Buckley, A. M., J. Wang, D. L. Hudson, A. J. Grant, M. A. Jones, D. J. Maskell, and M. P. Stevens. Evaluation of live-attenuated Salmonella vaccines expressing Campylobacter antigens for control of *C. jejuni* in poultry. Vaccine 28:1094–1105. 2010.

5. Carsiotis, M., D. L. Weinstein, H. Karch, I. A. Holder, and A. D. O'Brien. Flagella of *Salmonella* typhimurium are a virulence factor in infected C57BL/6J mice. Infect. Immun. 46:814–818. 1984.

6. Cogan, T. A., and T. J. Humphrey. The rise and fall of *Salmonella* Enteritidis in the UK. J. Appl. Microbiol. 94 (Suppl.):114S–119S. 2003.

7. Dey, A. K., and I. K. Srivastava. Novel adjuvants and delivery systems for enhancing immune responses induced by immunogens. Expert Rev. Vaccines 10:227–251. 2011.

8. Fukutome, K., S. Watarai, M. Mukamoto, and H. Kodama. Intestinal mucosal immune response in chickens following intraocular immunization with liposome-associated *Salmonella* enterica serovar enteritidis antigen. Dev. Comp. Immunol. 25:475–484. 2001.

9. Gomez-Verduzco, G., G. Tellez, A. L. Quintana, A. Isibasi, and V. Ortiz-Navarrete. Humoral immune response in breeding hens and protective immunity provided by administration of purified *Salmonella* Gallinarum porins. Poult. Sci. 89:495–500. 2010.

10. Hogue, A., P. White, J. Guard-Petter, W. Schlosser, R. Gast, E. Ebel, J. Farrar, T. Gomez, J. Madden, M. Madison, A. M. McNamara, R. Morales, D. Parham, P. Sparling, W. Sutherlin, and D. Swerdlow. Epidemiology and control of egg-associated *Salmonella enteritidis* in the United States of America. Rev. Sci. Tec. 16:542–553. 1997.

11. Kuehn, B. M. Salmonella cases traced to egg producers: findings trigger recall of more than 500 million eggs. J. Am. Med. Assoc. 304:1316. 2010.

12. Li, W., S. Watarai, T. Iwasaki, and H. Kodama. Suppression of *Salmonella enterica* serovar Enteritidis excretion by intraocular vaccination with fimbriae proteins incorporated in liposomes. Dev. Comp. Immunol. 28:29–38. 2004.

13. Little, C. L., S. Surman-Lee, M. Greenwood, F. J. Bolton, R. Elson, R. T. Mitchell, G. N. Nichols, S. K. Sagoo, E. J. Threlfall, L. R. Ward, I. A. Gillespie, and S. O'Brien. Public health investigations of *Salmonella* Enteritidis in catering raw shell eggs, 2002–2004. Lett. Appl. Microbiol. 44:595–601. 2007.

14. Lowry, O. H., N. Rosenbrough, A. L. Farr, and R. J. Randall. Protein measurement with the Folin phenol reagent. J. Biol. Chem. 193:265–275. 1951.

15. Min, W., H. S. Lillehoj, J. Burnside, K. C. Weining, P. Staeheli, and J. J. Zhu. Adjuvant effects of IL-1beta, IL-2, IL-8, IL-15, IFN-alpha, IFN-gamma TGF-beta4 and lymphotactin on DNA vaccination against *Eimeria acervulina*. Vaccine 20:267–274. 2001.

16. Mizel, S. B., and J. T. Bates. Flagellin as an adjuvant: cellular mechanisms and potential. J. Immunol. 185:5677–5682. 2010.

17. Mumma, G. A., P. M. Griffin, M. I. Meltzer, C. R. Braden, and R. V. Tauxe. Egg quality assurance programs and egg-associated *Salmonella enteritidis* infections, United States. Emerg. Infect. Dis. 10:1782–1789. 2004.

18. Okamura, M., H. S. Lillehoj, R. B. Raybourne, U. Babu, and R. Heckert. Antigen-specific lymphocyte proliferation and interleukin production in chickens immunized with killed *Salmonella enteritidis* vaccine or experimental subunit vaccines. Avian Dis. 47:1331–1338. 2003.

19. Okamura, M., H. S. Lillehoj, R. B. Raybourne, U. S. Babu, and R. A. Heckert. Cell-mediated immune responses to a killed *Salmonella enteritidis* vaccine: lymphocyte proliferation, T-cell changes and interleukin-6 (IL-6), IL-1, IL-2, and IFN-gamma production. Comp. Immunol. Microbiol. Infect. Dis. 27:255–272. 2004.

20. Okamura, M., M. Sonobe, S. Obara, T. Kubo, T. Nagai, M. Noguchi, K. Takehara, and M. Nakamura. Potential egg contamination by *Salmonella enterica* serovar Typhimurium definitive type 104 following experimental infection of pullets at the onset of lay. Poult. Sci. 89: 1629–1634. 2010.

21. Okamura, M., H. Tachizaki, T. Kubo, S. Kikuchi, A. Suzuki, K. Takehara, and M. Nakamura. Comparative evaluation of a bivalent killed Salmonella vaccine to prevent egg contamination with *Salmonella enterica* serovars Enteritidis, Typhimurium, and Gallinarum biovar Pullorum, using 4 different challenge models. Vaccine 25:4837–4844. 2007.

22. Pogonka, T., C. Klotz, F. Kovacs, and R. Lucius. A single dose of recombinant *Salmonella* typhimurium induces specific humoral immune responses against heterologous *Eimeria tenella* antigens in chicken. Int. J. Parasitol. 33:81–88. 2003.

23. Sheela, R. R., U. Babu, J. Mu, S. Elankumaran, D. A. Bautista, R. B. Raybourne, R. A. Heckert, and W. Song. Immune responses against *Salmonella enterica* serovar enteritidis infection in virally immunosuppressed chickens. Clin. Diagn. Lab. Immunol. 10:670–679. 2003.

24. Stecher, B., S. Hapfelmeier, C. Muller, M. Kremer, T. Stallmach, and W. D. Hardt. Flagella and chemotaxis are required for efficient induction of *Salmonella enterica* serovar Typhimurium colitis in streptomycin-pretreated mice. Infect. Immun. 72:4138–4150. 2004.

25. Toyota-Hanatani, Y., Y. Kyoumoto, E. Baba, T. Ekawa, H. Ohta, H. Tani, and K. Sasai. Importance of subunit vaccine antigen of major FliC antigenic site of Salmonella enteritidis II: a challenge trial. Vaccine 27:1680–1684. 2009.

ACKNOWLEDGMENT

The authors thank the students of the Laboratory of Zoonoses, Kitasato University School of Veterinary Medicine for their technical assistance for the animal experiments.

J Toxicol Pathol 2011; 24: 215–222

Original

Fetal and Neonatal Goiter in Cynomolgus Monkeys Following Administration of the Antithyroid Drug Thiamazole at High Doses to Dams During Pregnancy

Tsuyoshi Yoshikawa[1], Akiko Moriyama[1], Rinya Kodama[1], Yuji Sasaki[1], Tatsumi Sunagawa[1], Takanobu Okazaki[1], Asami Urashima[1], Yoshiro Nishida[1], Akihiro Arima[1], Ayumi Inoue[1], Takayuki Negishi[2], Yasuhiro Yoshikawa[3], Toshio Ihara[1], and Hiroshi Maeda[1]

[1] Drug Safety Research Laboratories, Shin Nippon Biomedical Laboratories, Ltd., 2438 Miyanoura, Kagoshima 891-1394, Japan
[2] Depertment of Chemistry and Biological Science, School of Science and Engineering, Aoyama Gakuin University, 5-10-1 Fuchinobe, Sagamihara, Kanagawa 229-8558, Japan
[3] Laboratory of Zoonoses, School of Veterinary Medicine, Kitasato University, 23-35-1 Higashi, Towada, Aomori 034-8628, Japan

Abstract: To evaluate morphologic alterations in the thyroid gland in the second generation in cynomolgus monkeys, pregnant dams were exposed to high doses of thiamazole. In Experiment A, dams received thiamazole intragastrically via a nasogastric catheter from gestation day (GD) 50 to GD 150 or on the day before delivery. Initially, the dose level was 20 mg/kg/day (10 mg/kg twice daily); however, the dose level was subsequently decreased to 5 mg/kg/day (2.5 mg/kg twice daily), since deteriorated general conditions were observed in two dams. Six out of seven neonates died on the day of birth. The cause of neonatal death was tracheal compression and suffocation from goiter. The transplacental exposure to thiamazole affected the fetal thyroid glands and induced goiter in all neonates. The surviving neonate was necropsied 767 days after discontinuation of thiamazole exposure and showed reversibility of the induced changes. In Experiment B, dams were intragastrically administered thiamazole at 5 mg/kg/day (2.5 mg/kg twice daily) for treatment periods from GDs 51 to 70, 71 to 90, 91 to 110, 111 to 130 and 131 to 150. All fetuses showed enlarged thyroid glands but were viable. Histopathologically, hypertrophy and/or hyperplastic appearance of the follicular epithelium of the thyroid gland was observed at the end of each treatment period. The most active appearance of the follicular epithelium, consisting of crowded pedunculated structure, was demonstrated at end of the treatment period from GD 131 to 150. This is the first report on the morphology of fetal and neonatal goiter in the cynomolgus monkey. (DOI: 10.1293/tox.24.215; J Toxicol Pathol 2011; 24: 215-222)

Key words: goiter, thiamazole, transplacental exposure, fetus, neonate, cynomolgus monkey

Introduction

Thiamazole, an antithyroid drug known as a synonym for methimazole, is a member of the thioamide group. It has been used for more than half a century to treat hyperthyroidism caused by Graves' disease[1], a condition in which the overactive thyroid gland produces excessive amounts of thyroid hormones. Thiamazole inhibits thyroid hormone synthesis stages, including the addition of iodine to thyroglobulin by the enzyme thyroperoxidase, which is essential to the synthesis of thyroxine. Thiamazole has been the drug of choice for treatment of hyperthyroidism during pregnancy and needs to be effectively managed and used to prevent maternal, fetal and neonatal complications. A literature review showed that infants born to mothers whose conditions had been managed with antithyroid drugs developed goiter[1-5]. However, there has been no report on the histopathology of goiter in nonhuman primate fetuses and neonates following administration of antithyroid drugs to dams. In the present study, we repeatedly administered relatively high doses of thiamazole to pregnant cynomolgus monkeys in the second and third trimesters of pregnancy to examine thyroidal morphological disorders in fetuses and neonates.

Received: 16 June 2011, Accepted: 23 August 2011
Mailing address: Tsuyoshi Yoshikawa, Pathology Department, Shin Nippon Biomedical Laboratories, Ltd., 2438 Miyanoura, Kagoshima 891-1394, Japan
TEL: 81-99-294-2600 FAX: 81-99-294-3619
E-mail: yoshikawa-tsuyoshi@snbl.co.jp
©2011 The Japanese Society of Toxicologic Pathology
This is an open-access article distributed under the terms of the Creative Commons Attribution Non-Commercial No Derivatives (by-nc-nd) License <http://creativecommons.org/licenses/by-nc-nd/3.0/>.

Materials and Methods

Animals and housing conditions

Adult female cynomolgus monkeys (*Macaca fascicularis*, age 3 to 8 years, body weight 2.6–5.4 kg, purpose bred) from China maintained in the primate facility of Drug Safety Research Laboratories, Shin Nippon Biomedical Laboratories, Ltd. (SNBL DSR), were used. Dams and offspring (after weaning) were individually provided with approximately 108 g (approximately 12 g × 9 pieces) and 72 g (approximately 12 g × 6 pieces), respectively, of solid food (Teklad Global Certified 25% Protein Primate Diet, Harlan Sprague Dawley, Inc., Madison, WI, USA) once daily between 14:30 and 16:00. Any remaining food was removed between 08:30 and 10:00 on the following day. Water conforming to the water quality standards required by the Japanese Waterworks Law was available *ad libitum* from an automatic supply (Edstrom Industries, Inc., Waterford, WI, USA). Stainless steel animal cages (Taiyo Stainless Co., Ltd., Kagoshima, Japan) conforming to USDA standards [690 mm (D) × 610 mm (W) × 750 mm (H)] were used. The number of animals per cage was one. Males and females were housed in pairs during the mating period. The animal rooms were maintained at a temperature of 23 °C to 29 °C and humidity of 35% to 75%, with artificial lightning for 12 hours/day (06:00 to 18:00). The use of animals in this study was approved by the Institutional Animal Care and Use Committee of SNBL DSR, and the study was performed in accordance with the ethics criteria contained in the bylaws of the committee.

Mating and pregnancy diagnosis

Females that showed regular menstrual cycles were mated with males of proven fertility for three days between the 11th and 15th days of the menstrual cycle. When copulation was confirmed visually, the median day of the mating period was designated as gestation day 0 (GD 0). On presumed GD 18, pregnancy was diagnosed by ultrasonography (SSD-4000, Hitachi-Aloka Medical, Ltd., Tokyo, Japan) under sedation from an intramuscular injection of 10 mg/kg of ketamine hydrochloride (Fuji Chemical Industry Co., Ltd., Saitama, Japan). Animal numbers were allotted in the order in which it was possible to confirm pregnancy (Experiment A or B). Thereafter, pregnant animals underwent treatment with one of the dosing regimens stated below.

Treatment of dams

Experiment A: Ten dams received thiamazole (Sigma-Aldrich Co., Ltd., Tokyo, Japan) intragastrically via a nasogastric catheter from GD 50 to GD 150 or on the day before delivery. Initially, the dose level was 20 mg/kg/day (10 mg/kg twice daily); however, the dose level was subsequently decreased to 5 mg/kg/day (2.5 mg/kg twice daily), since deteriorated general conditions were observed in two dams. Thiamazole was administered twice a day, and the second administration was 6 hours after the first. All dams were observed four times a day during the treatment period and once a day during the nontreatment period and were to be allowed to deliver naturally.

Experiment B: Two dams per group were administered thiamazole (Sigma-Aldrich) at 5 mg/kg/day (2.5 mg/kg twice daily) intragastrically via a nasogastric catheter for one of five different treatment periods. Thiamazole was administered twice a day, and the second administration was 6 hours after the first. Two or three animals were allocated to Groups 1, 2, 3, 4 and 5 as nontreated controls. The treatment periods for Groups 1, 2, 3, 4 and 5 were GDs 51 to 70, 71 to 90, 91 to 110, 111 to 130 and 131 to 150, respectively. All dams were observed four times a day during the treatment period and once a day during the nontreatment period. Cesarean section (CS) was performed on the day following the end of the relevant treatment period, and the treated fetuses were removed from the uterus.

Observations and examinations of second generation

All neonates were examined for viability, sex, body weight and external findings at birth. The offspring of Dam No. 7 in Experiment A was necropsied 767 days after birth. The thyroid glands collected from fetuses in Experiment B were weighed, and absolute and relative weights were calculated from the relevant fetal body weight. The fetal and neonatal thyroid glands from Experiments A and B were fixed in 10% neutral buffered formalin for histopathological examination. The specimens were embedded in paraffin, sectioned and stained routinely with Hematoxylin-Eosin (HE) stain. Slide specimens were examined microscopically. Neonates No.3 and No.7 in Experiment A and all treated fetuses and one nontreated fetus from each group in Experiment B were available for histopathological examination.

Examination of morphological parameters in the thyroid gland in Experiment B

Images of the thyroid were analyzed with analysis (Soft Imaging System GmbH, Muenster, Germany) software to determine the height of the follicular epithelium. The outer circumferences of the follicle and the lumen included in a one square millimeter section of each specimen were measured. The average radius and diameter of each were then calculated. The height of the follicular epithelium was calculated by subtracting the lumen radius from the follicular radius. Pairwise comparisons were performed for each parameter by t-test based on a one-way ANOVA model. A value of $p<0.05$ was considered statistically significant.

Results

Experiment A

Clinical signs in dams and the viability outcomes for fetuses and neonates are shown in Table 1. Two dams (Nos. 1 and 2) showed convulsion, prone position, external genital bleeding and/or low food consumption, and one of these dams (No. 1) then died on GD 70 and the other dam (No. 2) aborted its fetus. Therefore, the dose level of thiamazole was decreased from 20 mg/kg/day (10 mg/kg twice daily) to

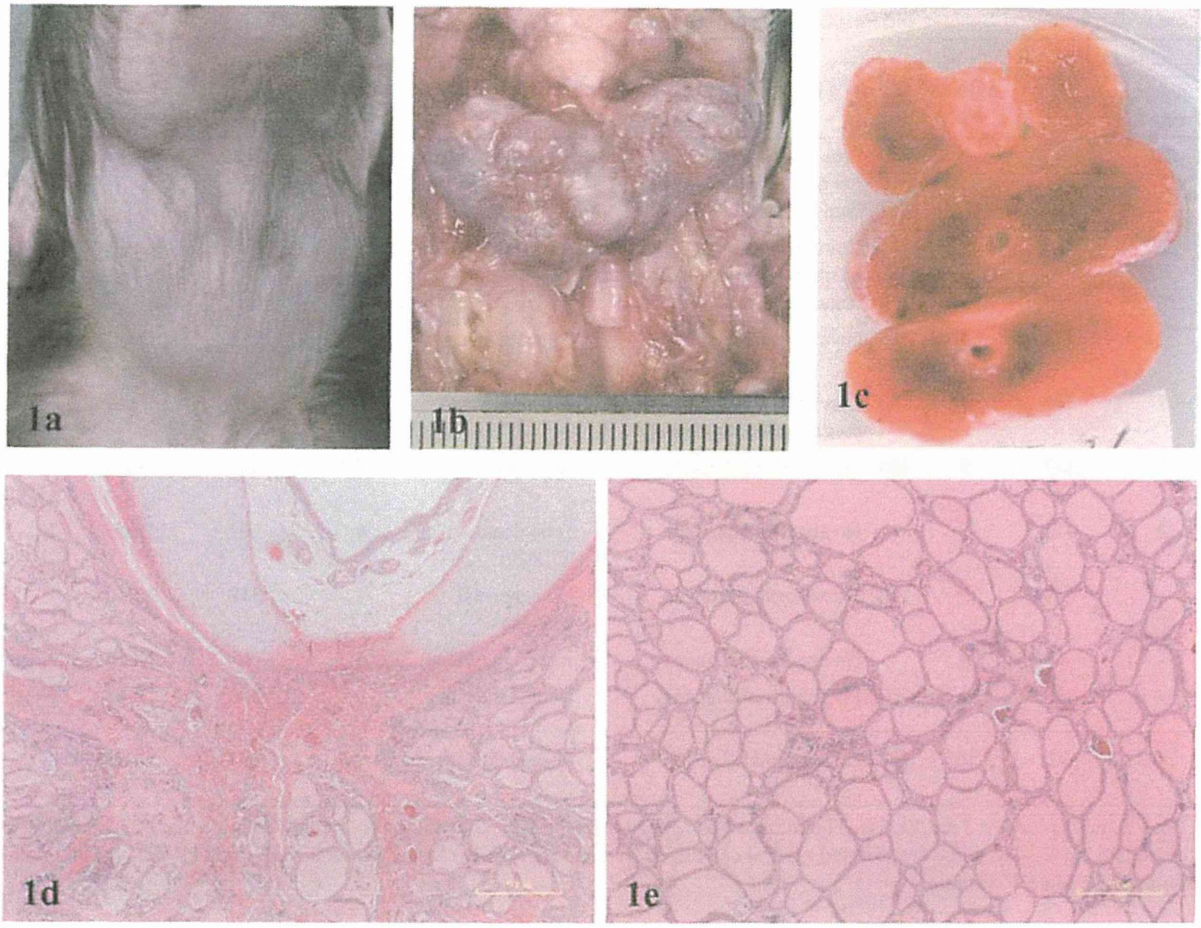

Fig. 1. Gross and histopathological findings in neonates in Experiment A. 1a: External appearance around the neck. 1b: Gross appearance of the thyroid gland. 1c: Cut surface of the thyroid gland. 1d: Thyroid gland reached the membranous wall of the trachea, HE stain. 1e: Follicles consisted of a flattened epithelium containing colloid, HE stain.

5 mg/kg/day (2.5 mg/kg twice daily). After the decrease in dose level, one other dam (No. 4) showed low body weight, low food consumption and emaciation; however, this dam was able to maintain its pregnancy until the end of the third trimester, and no abnormalities in clinical signs were observed in the other seven dams (Nos. 3 and 5 to 10). At around the end of the gestation period, fetal death (No. 6) was detected by ultrasonography on GD 170, and six other dams (Nos. 3, 4, 5, 7, 9 and 10) were able to deliver naturally. However, five out of the six neonates (Nos. 3, 4, 5, 9 and 10) died on the day of birth, and only one neonate (No. 7) survived. All fetuses and neonates that had been viable at the end of the third trimester showed swollen throat and presented palpable thyroid glands. Gross examination of this fetus and these neonates showed enlarged thyroid glands reaching the membranous wall of the trachea. Histopathologically, the thyroid showed colloid storage and a flattened follicular epithelium. Neither cellular atypia nor mitotic figures were seen (Figs. 1a-e). The offspring (No. 7) necropsied 767 days after birth showed no macroscopic abnormalities in the thyroid gland. Histopathologically, deposition of brown pigment and proliferation of connective tissue were observed in this animal; however, no abnormal changes were observed in the follicular epithelium. Absolute and relative thyroid gland weights in this offspring were 1.42 g and 0.81 g/kg (body weight at necropsy: 1.76 kg), respectively.

Experiment B

The results of Experiment B are shown in Tables 2 and 3. No abortion or fetal death occurred during any thiamazole treatment period. All fetuses removed from uteri by cesarean section were viable. There was no difference in body weight between the control fetuses and the treated fetuses. All treated fetuses from Groups 1 to 5 showed enlarged thyroid glands (Fig. 2a–e). Absolute and relative thyroid weights in the treated fetuses were higher than those in the control fetuses. The follicular diameters, lumen diameters and the heights of the follicular epithelium were significantly higher in treated fetuses than control fetuses. Although the height of the follicular epithelium did not show any apparent increase, the follicular diameter and lumen di-

Table 1. Experimental Designs and Results of Experiment A

Thiamazole[a]		Dam animal No.	GD	Clinical signs of dams	Delivery status	Neonate animal No.	Body weight at birth (g)	Viability	Sex	External findings
20 mg/kg Treated period (days)	5 mg/kg									
20	-	1	-	Prone position (GD69), external genital bleeding (GD70), dam death (GD70)	Abortion (GD70)	1	NE	Dead	NE	NE
33	-	2	-	Convulsion (GD69-71), prone position (GD69), low food consumption (GD70~)	Abortion (GD83)	2	NE	Dead	NE	NE
7	108	3	165	No abnormal changes	Neonatal death	3	245	Dead	M	Swelling, throat
7	111	4	168	Low body weight, low food consumption, emaciation	Neonatal death	4	249	Dead	M	Swelling, throat
3	127	5	180	No abnormal changes	Neonatal death	5	320	Dead	F	Swelling, throat
2	118	6	-	No abnormal changes	Fetal death (GD170)	6	NE	Dead	F	Swelling, throat
-	118	7	168	No abnormal changes	No abnormal changes	7	331	Alive	F	Swelling, throat
-	40	8	-	No abnormal changes	Abortion (GD90)	8	NE	Dead	NE	NE
-	120	9	170	No abnormal changes	Neonatal death	9	302	Dead	F	Swelling, throat
-	92	10	142	No abnormal changes	Neonatal death	10	197	Dead	M	Swelling, throat

[a] Dose 20 mg/kg/day → 5 mg/kg/day. Thiamazole was administered on GD 50 to 150 or on the day before delivery. The dose level was decreased to 5 mg/kg/day, since deteriorated general conditions were observed in two dams (Animal Nos. 1 and 2). GD: Gestation day. NE: Not examined. M: Male. F: Female.

ameter tended to increase as gestation progressed.

The histopathological appearances of the thyroid glands from each group are shown in Figs. 3a to 3e'. Mitotic figures were sporadically observed in the follicular epithelium in treated fetuses from all groups. Hypertrophy and/or hyperplasia of the thyroid follicular epithelium were diffusely observed in treated fetuses from all groups. Follicular size was distinctly larger in the treated fetuses than in the control fetuses, with narrowed lumens. The follicular cells were more columnar than normal. Control thyroid glands examined at GD 72 and GD 91 consisted of a number of small follicles thought to be immature. Projections into the follicular lumen as a result of proliferation of the follicular epithelium were observed at GD 91. Large follicles lined by a low cuboidal follicular epithelium were observed at GD 131. The follicular epithelium showed an active appearance with proliferated papillary projections into the follicular lumen and pedunculated structure at GD 151.

Discussion

Experiment A, thiamazole was administered at relatively high doses for an antithyroid drug to pregnant cynomolgus monkeys during pregnancy to investigate morphologic changes in fetuses and neonates. In Experiment B, morphologic changes in the fetal thyroid glands during the second and third trimesters were investigated sequentially with five different treatment periods to examine the effect of thiamazole. It has been reported that the drug induced hypertrophy of the follicular epithelium in the thyroid glands of common marmosets (*Callithrix jacchus*)[6]. However, there has been no report of histopathological changes in nonhuman primate fetuses and neonates until now. The thyroid glands from fetuses exposed to thiamazole during the second and third trimesters of pregnancy were compared morphologically with those from control fetuses.

The thyroid gland is one of the organs most susceptible to various intrinsic and extrinsic factors[7], and the hypothalamus-pituitary-thyroid axis and its hormonal feedback system involving TSH, triiodothyronine (T3) and thyroxine (T4) is well established.

Thiamazole, an antithyroid drug, is a member of the thioamide group. Thiamazole (1-methy-1*H*-imidazole-2-thiol), whose chemical formula is $C_4H_6N_2S$ and whose molecular mass is 114.17 g/mol has been used for more than half a century to treat hyperthyroidism caused by Graves' disease[1], a condition in which the overactive thyroid gland produces excessive amounts of thyroid hormones. The working mechanism of thiamazole is based on inhibition of the addition of iodine to thyroglobulin by the enzyme thyroperoxidase, an essential step in the synthesis of T3 and T4.

It has been reported that thionamide compounds are

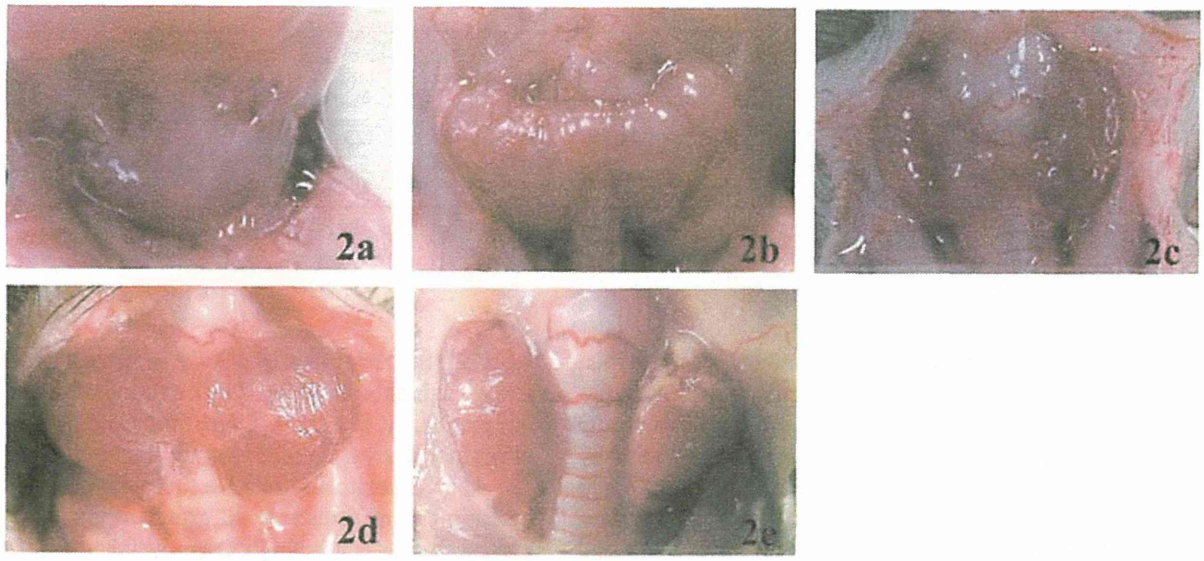

Fig. 2. Gross appearance of changes in the thyroid glands of fetuses in Experiment B with 5 different treatment periods. All fetuses in thiamazole exposure Groups 1 to 5 showed swollen throats. 2a: Treatment period GD 51 to 70; fetuses removed on Day 71. 2b: Treatment period was GD 71 to 90; fetuses removed on Day 92. 2c: Treatment period GD 91 to 110; fetuses removed on Day 111. 2d: Treatment period GD 111 to 130; fetuses removed on Day 131. 2e: Treatment period GD 131 to 150; fetuses removed on Day 151.

Table 2. Experimental Designs and Results of Experiment B

Group	Dam animal No.	Dose (mg/kg)	Dosing days (GD)	CS* day	Neonate animal No.	Viability	Sex	Fetal weight (g)	Organ weight (Thyroid)	
									Absolute weight (mg)	Relative weight (mg/g)
1	Control-1	-	-	72	Control-1	Alive	F	33.1	13.0	0.39
	Control-2		-	72	Control-2		M	22.3	5.4	0.24
	101	5	51–70	71	101		F	33.8	135.0	3.99
	102			71	102		F	32.4	180.0	5.56
2	Control-3	-	-	91	Control-3		M	84.2	18.0	0.21
	Control-4		-	91	Control-4		M	77.1	27.6	0.36
	201	5	71–90	91	201		M	61.0	185.4	3.04
	202			92	202		M	89.7	531.8	5.93
3	Control-5	-	-	110	Control-5		M	165.0	64.0	0.39
	Control-6		-	110	Control-6		M	157.5	48.3	0.31
	Control-7		-	111	Control-7		M	150.5	30.3	0.20
	301	5	91–110	110	301		F	170.0	360.0	2.12
	302			111	302		M	162.0	316.0	1.95
4	Control-8	-	-	131	Control-8		M	228.5	56.0	0.25
	Control-9		-	131	Control-9		M	273.2	123.2	0.45
	401	5	111–130	131	401		F	256.3	840.0	3.28
	402			131	402		M	260.5	341.0	1.31
5	Control-10	-	-	151	Control-10		M	307.4	50.0	0.16
	Control-11		-	155	Control-11		F	363.0	147.0	0.40
	501	5	131–150	152	501		M	332.4	560.0	1.68
	502			151	502		F	363.9	533.5	1.47

GD: Gestation day. M: Male. F: Female. *: Caesarean section.

among the most potent inhibitors of thyroid hormones and that they have induced hyperplasia of the thyroid gland in experimental animals[8]. This effect occurs when the administration of the drug reduces thyroid hormones to subnormal levels and the resultant increase in circulating TSH stimulates enlargement of the thyroid gland.

The cynomolgus monkey, a widely used nonhuman primate model, has similar reproductive physiology, endo-

Table 3. Morphological Parameters in the Thyroid Gland in Experiment B

Group	1		2		3		4		5	
Dose (mg/kg)	-	5	-	5	-	5	-	5	-	5
Dosing days (GD)	-	51–70	-	71–90	-	91–110	-	111–130	-	131–150
Follicular diameter (μm)	36.09	89.53*	44.25	115.71*	69.35	123.45*	96.85	156.16*	65.90	164.13*
Lumen diameter (μm)	27.29	56.15*	35.47	83.49*	54.75	86.17*	77.99	123.96*	47.36	128.19*
Height of follicular epithelium (μm)	4.40	16.69*	4.39	16.11*	7.30	18.64*	9.43	16.10*	9.27	17.97*

GD: Gestation day. Values are expressed as averages. *: Significantly different from the control (P<0.05).

crinology and development to the human[9,10]. The human gestation period is around 40 weeks, while that of the cynomolgus monkey is around 160 days[10]. Organogenesis occurs during the first trimester in both the cynomolgus monkey and the human, between GDs 21 and 50 and GDs 18 and 60, respectively[9,10]. It has been reported that the development of the human thyroid gland begins from GD 21[11], and that the human thyroid gland is well developed by GD 70 in the first trimester and begins concentrating iodide and producing thyroid hormones at this time[11]. Compounds with a molecular weight greater than 1000 Da do not cross the placenta easily, whereas those of less than 600 Da, including thiamazole, freely cross the placenta[2–4,12–14]. In the present study, an excessive dosage of thiamazole affected the fetal thyroid glands through the placenta, inducing goiter in fetuses or neonates.

Fetal, neonatal or maternal death or abortion occurred in Experiment A. It was considered that the cause of death was respiratory impairment following severe compression of the trachea by an enlarged thyroid gland, as has been reported in humans[1,2]. Compression of the cervical region by an excessively enlarged thyroid gland is considered potentially lethal to neonates.

One offspring (No. 7), which showed a swollen throat at birth, was necropsied on Day 767. Although no abnormal changes were observed macroscopically, its absolute thyroid gland weight was above the range of the control background data (unpublished data) of our laboratories. This organ weight result in this animal showed that even at the age of two years, thyroid gland weights had not returned to normal, a finding similar to that reported in rats[15]. Moreover, there were no abnormal changes in the follicular cells. Histopathological changes observed in the interstitium of the thyroid gland were considered traces of goiter at birth. Regression of goiter induced in fetuses was observed when antithyroid compounds including propylthiouracil (PTU) were withdrawn, enabling reversibility of the induced changes[2,15,16].

In Experiment B, there were no nonviable outcomes for fetuses or abnormalities in fetal body weight. All treated fetuses from each group that underwent treatment for one of five periods showed goiter. The detection of fetal goiter during pregnancy in a mother on antithyroid drug therapy by ultrasonography is an indication of fetal hypothyroidism[1–3].

High absolute and relative thyroid organ weights were noted in treated fetuses in all groups when compared with control fetuses. These high organ weights were considered to be due to the increase in size of the follicle and the colloid, since both the follicular and lumen diameters increased as gestation progressed.

Although the mean height of the follicular epithelium in the treated groups did not show any apparent increase in morphometry examinations, both diffuse hyperplasia and hypertrophy of the thyroid follicular epithelium were observed in the histopathological examination. In Group 4 (GD 111 to 130 treatment period), around the midpoint of the third trimester, an inactive appearance of the follicular epithelium was seen. This was considered to indicate that the susceptibility to thiamazole in this group was not as great as in the other groups. In contrast to those from Group 4 (GD 111 to 130 treatment period), the fetal thyroids from Group 5 (GD 131 to 150 treatment period) demonstrated the most characteristic appearance of thiamazole treatment-related changes. The follicular epithelium appeared active, consisting of papillary projections into the follicular lumens that had become pedunculated. This observation suggests that administration of thiamazole to dams just before delivery strongly induces histopathological changes in the follicular epithelium of the thyroid gland in the fetal cynomolgus monkey. Although TSH and thyroid hormones were not assessed in the present study, the morphologic features of the thyroid glands from treated fetuses were consistent with enhanced resorption of colloid through TSH stimulation[17].

In conclusion, this is the first report on macroscopic and histopathological investigations of goiter in cynomolgus monkey fetuses and neonates when dams received relatively high doses of thiamazole during the second and third trimesters of pregnancy.

Fig. 3. Histologic appearance of changes in the thyroid glands of fetuses in Experiment B with 5 different treatment periods, HE stain. 3a: Induced change in the thyroid gland at GD 71. 3a': Control thyroid gland at GD 72. 3b: Induced change in the thyroid gland at GD 91. 3b': Control thyroid gland at GD 91. 3c: Induced change in the thyroid gland at GD 111. 3c': Control change in the thyroid gland at GD 111. 3d: Induced change in the thyroid gland at GD 131. 3d': Control thyroid gland at GD 131. 3e: Induced change in the thyroid gland at GD 151. 3e': Control thyroid gland at GD 151.

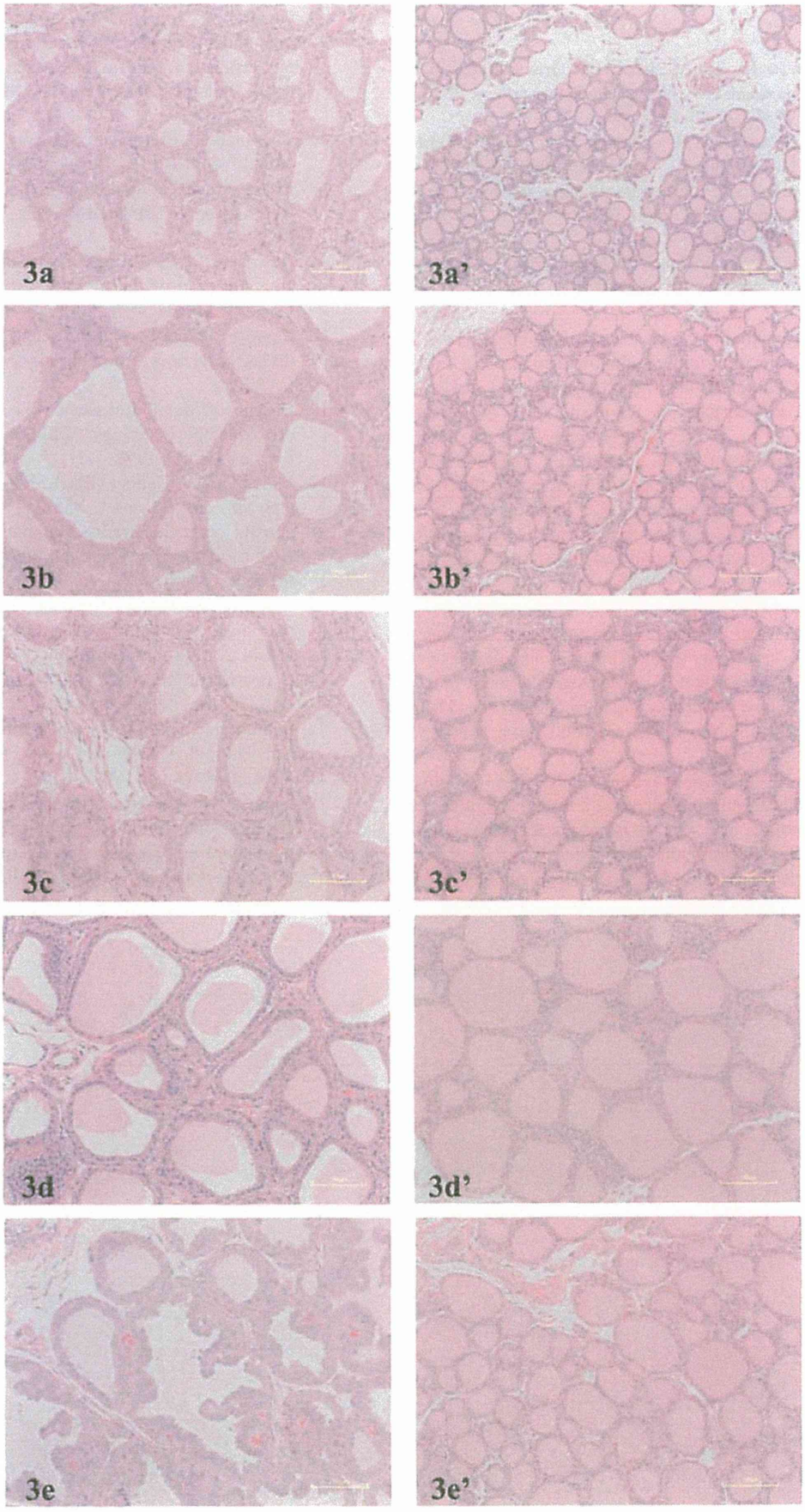

Fig. 3.

References

1. Patil-Sisodia K, and Mestman JH. Graves hyperthyroidism and pregnancy: A clinical update. Endocra Pract. **16**: 118–129. 2010. [Medline] [CrossRef]
2. Miyata I, Abe-Gotyo N, Tajima A, Yoshikawa H, Teramoto S, Seo M, Kanno K, Sugiura K, Tanaka T, and Eto Y. Successful intrauterine therapy for fetal goitrous hypothyroidism during late gestation. Endocr J. **54**: 813–817. 2007. [Medline] [CrossRef]
3. Luton D, La Gac I, Vuillard E, Castanet M, Guibourdenche J, Noel M, Toubert ME, Leger J, Boissinot C, Schlageter MH, Garel C, Tebeka B, Oury JF, Czernichow P, and Polak M. Management of Graves' disease during pregnancy: The key role of fetal thyroid gland monitoring. J Clin Endocrinol Metab. **90**: 6093–6098. 2005. [Medline] [CrossRef]
4. Laurberg P, Bournaud C, Karmisholt J, and Orgiazzi J. Management of Graves' disease in pregnancy: focus on both maternal and foetal thyroid function, and caution against surgical thyroidectomy in pregnancy. Eur J Endocrinol. **160**: 1–8. 2009. [Medline] [CrossRef]
5. Cunningham AR, Carrasquer CA, and Mattison DR. A categorical structure–activity relationship analysis of the developmental toxicity of antithyroid drugs. Int J Pediatr Endocrinol. **2009**: 936154. 2009. [Medline] [CrossRef]
6. Kurata Y, Wako Y, Tanaka K, Inoue Y, and Makinodan F. Thyroid hyperactivity induced by methimazole, spironolactone and phenobarbital in marmosets (*Callithrix jacchus*): Histopathology, plasma thyroid hormone levels and hepatic T_4 metabolism. J Vet Med Sci. **62**: 607–614. 2000. [Medline] [CrossRef]
7. Ishida K, Narita K, Ito K, Izumisawa N, Nii A, Okamiya H, and Hanada T. Morphologic variations in the thyroid glands of cynomolgus monkeys (*Macaca fascicularis*). J Toxicol Pathol. **13**: 189–191. 2000. [CrossRef]
8. Greaves P. Endocrine glands. In: Histopathology of Preclinical Toxicity Studies, 3rd ed. Elsevier, Amsterdam. 830. 2007.
9. Graham CE. Reproductive and developmental toxicology in nonhuman primates. In: Preclinical Safety of Biotechnology Products Intended For Human Use (Progress in Clinical & Biological Research). Alan R Liss, Inc., New York. 73–88. 1987.
10. Chellman GJ, Bussiere JL, Makori N, Martin PL, Ooshima Y, and Weinbauer GF. Developmental and reproductive toxicology studies in nonhuman primates. Birth Defects Res B Dev Reprod Toxicl. **86**: 446–462. 2009. [Medline] [CrossRef]
11. Howdeshell KL. A model of the development of the brain as a construct of the thyroid system. Environmen Health Perspect. **110**: 337–348. 2002. [Medline] [CrossRef]
12. Inoue M, Arata N, Koren G, and Ito S. Hyperthyroidism during pregnancy. Can Fam Physician. **55**: 701–703. 2009. [Medline]
13. Haschek WM, and Rousseaux CG. Fetus. In: Fundamentals of Toxicologic Pathology. Academic Press, San Diego, California. 521–522. 1998.
14. Mortimer RH, Cannel GR, Addison RS, Johnson LP, Roberts MS, and Bernus I. Methimazole and propylthioracil equally cross the perfused human term placental lobule. J Clin Endocrinol Metab. **82**: 3099–3102. 1997. [Medline] [CrossRef]
15. Todd GC. Induction and reversibility of thyroid proliferative changes in rats given an antithyroid compound. Vet Pathol. **23**: 110–117. 1986. [Medline] [CrossRef]
16. Ochoa-Maya MR, Frates MC, Lee-Parritz A, and Seely EW. Resolution of fetal goiter after discontinuation of propylthiouracil in a pregnant woman with Graves' hyperthyroidism. Thyroid. **9**: 1111–1114. 1999. [Medline] [CrossRef]
17. Reindel JF, Gough AW, Pilcher GD, Bobrowski WF, Sobocinski GP, and De La Iglesia FA. Systemic proliferative changes and clinical signs in cynomolgus monkeys administered a recombinant derivative of human epidermal growth factor. Toxicol Pathol. **29**: 159–173. 2001. [Medline] [CrossRef]

Comparative Medicine
Copyright 2012
by the American Association for Laboratory Animal Science

Vol 62, No 1
February 2012
Pages 53–60

Original Research

Differentiation of Neural Cells in the Fetal Cerebral Cortex of Cynomolgus Monkeys (*Macaca fascicularis*)

Yujiro Toyoshima,[1,*] Satoshi Sekiguchi,[1] Takayuki Negishi,[3] Shinichiro Nakamura,[4] Toshio Ihara,[5] Yoshiyuki Ishii,[1] Shigeru Kyuwa,[1] Yasuhiro Yoshikawa,[1,6] and Kimimasa Takahashi[2]

Proliferation and programmed cell death are important in the formation of morphologic structures and functional activity during CNS development. We used immunohistochemical and TUNEL methods to examine the proliferation and differentiation of neural cells in, distribution of apoptotic cells in, and microglial cell involvement in the removal of apoptotic cells from the fetal cerebral cortex of cynomolgus monkeys. At embryonic day (E) 50 and E80, the neuroepithelium contained many mitotic cells. Cells staining for PCNA (a nuclear marker of proliferating cells) were prominent in the proliferative zone, whereas cells positive for NeuN (a neuron-specific marker) were absent. GFAP staining for glial cells was positive in the neuroepithelium and radial glial fibers. Iba1-positive cells (that is, macrophages and microglia) were distributed throughout all regions at all time points but accumulated especially in the ventricular zone at E80. Apoptotic morphology (at E80) and TUNEL-positive cells (that is, containing DNA fragmentation; at E50 and E80) were observed also. At E120 and E150, most PCNA-positive cells were in the ventricular zone, and NeuN-positive cells were prominent in all layers except layer I-II at E120. GFAP immunoreactivity was detected mainly in cells with fine processes in the white matter. Neither apoptosis nor TUNEL-positive cells were detected at either E120 or E150. These results suggest that proliferation, migration, and neural cell death occur during midgestation (that is, E50 to E80) in fetal brain of cynomolgus macaques, whereas differentiation and maturation of neural cells occur after midgestation (E80).

Abbreviations: E, embryonic day; GW, gestational week; PCD, programmed cell death.

The proliferation and programmed cell death (PCD) of neural cells during development of the CNS are important in the formation of morphologic structures and functional activity of the brain.[4,26,35] In normal corticogenesis, neuronal and glial precursors proliferate in the neuroepithelium covering the ventricle, and postmitotic neuronal precursors migrate to the cortical plate as their final destination. During this process, radial glial cells guide migrating cells. Neuronal precursors that have completed migration differentiate into mature neurons to form cerebral cortical layers.[25] During cortical developmental processes, PCD—mainly apoptosis—emerges. PCD reportedly occurs during corticogenesis at early to mid-pregnancy in humans[1,6,26,31] but between embryogenesis and the postnatal period in rodents.[3,4] In addition, microglia infiltration emerges to remove cells that have undergone PCD.[10,26] Some reports, however, suggest that the distribution of microglia is not always correlated with PCD.[2,27] Therefore, microglial involvement in PCD has not been confirmed during fetal brain development. Moreover, PCD has often been described during cerebral development in humans and rodents, but few reports have examined PCD in monkeys.[13]

In the current study, we investigated the proliferation, differentiation, and distribution of apoptosis of neural cells in the fetal brain, especially the cerebral cortex, cynomolgus monkey at different developmental stages using histopathologic analysis, immunohistochemistry, and TUNEL method. In addition, we investigated the involvement of microglial infiltration in the removal of apoptotic cells from the fetal monkey brain.

Received: 28 Jun 2011. Revision requested: 29 Jul 2011. Accepted: 13 Aug 2011.
[1]Department of Biomedical Science, Graduate School of Agricultural and Life Sciences, The University of Tokyo, Tokyo, Japan; [2]Department of Veterinary Pathology, Nippon Veterinary and Life Science University, Musashino City, Tokyo, Japan; [3]Department of Chemistry and Biological Science, Aoyama Gakuin University, Sagamihara City, Kanagawa, Japan; [4]Research Center for Animal Life Science, Shiga University of Medical Science, Hikone City, Shiga, Japan; [5]Drug Safety Research Laboratory, Shin Nippon Biomedical Laboratories, Kagoshima City, Kagoshima, Japan; and [6]Laboratory of Zoonosis Control, College of Veterinary Medicine, Kitasato University, Towada City, Aomori, Japan.
[*]Corresponding author. Email: aa077150@mail.ecc.u-tokyo.ac.jp

Materials and Methods

Animals. Four pregnant cynomolgus monkeys (*Macaca fascicularis*) at gestational days 50, 80, 120, and 150 ($n = 1$ at each stage) were purchased from and maintained at Shin Nippon Biochemical Laboratories (Kagoshima City, Japan). Serologically normal monkeys that were imported from China and had passed quarantine were used in the present study. Animal breeding, mating, and operations were performed at Shin Nippon Biochemical Laboratories. In particular, female monkeys with normal menstrual cycles each were caged for 3 d with a healthy male monkey

during the time of expected ovulation. After an observer confirmed copulation or intravaginal sperm, the second of the 3 mating days was defined as gestational day 0. All monkeys were housed according to ILAR guidelines in individual stainless steel cages (69 × 61 × 75 cm) at 26 ± 2 °C and 50% ± 10% humidity, on a 12:12-h light:dark cycle, and with 15 fresh-air changes hourly.[16] Each monkey received about 108 g of food pellets once daily and had free access to drinking water.

After normal pregnancies were confirmed by ultrasonography, fetuses were obtained by Caesarean surgery, were confirmed alive, were euthanized by pentobarbital through the umbilical vein, and underwent autopsy. Dams received ampicillin (Meiji Seika Pharma, Tokyo, Japan) and buprenorphine hydrochloride (Otsuka Pharmaceutical, Tokyo, Japan) intramuscularly for 3 d postoperatively, and the surgical site was disinfected daily for 1 wk after surgery. In the current study, fetal cerebra at embryonic day (E) E50, E80, E120, and E150 were fixed in 4% paraformaldehyde or Bouin solution and embedded in paraffin. Coronal sections (E80, E120, and E150) of the occipital lobe and sagittal sections (E50) of the whole brain were sliced at 2 µm and stained with hematoxylin and eosin for histopathologic examination.

This study was performed according to guidelines for animal experiments at Shin Nippon Biomedical Laboratories. All procedures and protocols were approved by the Animal Care and Use Committee of the Graduate School of Agricultural and Life Sciences, the University of Tokyo.

Immunohistochemistry. Immunostaining was performed by the labeled streptavidin–biotin method for rabbit polyclonal antibodies[12] and by the polymer-based method for mouse monoclonal antibodies.[29] Deparaffinized sections were treated with 0.3% H_2O_2 in methanol for 30 min to block endogenous peroxidase activity in the tissue. After being washed in PBS, sections were autoclaved for 10 min at 121 °C to enhance immunoreactivity. The sections were incubated with Block Ace (DS pharma Biomedical, Osaka, Japan) for 1 h at room temperature, to prevent nonspecific binding of immunoglobulin. Tissue sections then were incubated overnight with primary antibodies against PCNA (proliferating cell nuclear antigen), a marker for cells in early G1 phase and S phase of the cell cycle (1:200; Dako, Glostrup, Denmark); NeuN, a marker of mature neurons (1:200; Chemicon International, Temecula, CA); GFAP (glial fibrillary acidic protein) a marker for neuroepithelium, radial glial fibers, and astroglia (1:1000; Dako); and Iba 1 (ionized calcium binding adapter molecule 1), a marker of macrophage and micloglia (1:1000; Wako, Osaka, Japan). For rabbit polyclonal antibodies, sections were incubated with biotinylated goat antirabbit IgG (1:500; Dako) for 30 min at 37 °C, followed by incubation with horseradish-peroxidase–conjugated streptavidin (1:500; Dako) for 30 min at room temperature. For mouse monoclonal antibodies, sections were incubated with EnVision+ (Dako) for 30 min at room temperature. Immunoreactivity was visualized by treating sections with 3, 3′-diaminobenzidine tetraoxide (Dojin Kagaku, Kumamoto, Japan). Sections were counterstained with hematoxylin or 0.1% methyl green.

Detection of apoptosis. Apoptosis was detected by TUNEL analysis (Apop Tag Peroxidase In Situ Apoptosis Detection Kit, Chemicon)[11] and immunohistochemistry using a rabbit polyclonal antibody against cleaved caspase 3 (1:50; Chemicon). TUNEL analysis was performed according to the manufacturer's protocol with minor modifications; for example, sections were pretreated with 1 µg/mL proteinase K (Wako) in PBS for 10 min at room temperature. Negative control sections were incubated with PBS as a substitute for terminal deoxynucleotidyl transferase. Caspase 3 immunohistochemistry was done as described earlier, except that Tris-buffered saline was substituted for PBS and a polymer-based detection method (EnVision+, Dako) was used.

Cell counts. TUNEL-, PCNA-, and NeuN-positive cells in each section at E50, E80, E120, and E150 were counted cells under light microscopy at 400× magnification. For E50 and E80, we focused on 3 layers: the cortical plate (including the marginal zone); intermediate zone; and proliferative zone (comprising the ventricular and subventricular zones). For E120 and E150, we evaluated 5 layers (namely, layers I-II, III, IV, V, and VI). After 5 random fields (1000 cells each) from each section were captured by using a CCD camera (Q Capture Pro; Nippon Roper, Tokyo, Japan), the number of positive cells per 1000 cells was computed by using Scion Image (Scion Corporation, Frederick, MD).

Results

Differentiation of neural cells at E50 and E80. Histologically, the cerebral wall included 5 areas: the ventricular zone, subventricular zone, intermediate zone, cortical plate, and marginal zone. At E80, the proliferative zone, which comprises the ventricular and subventricular zones, was slightly smaller and intermediate zone and cortical plate were larger than those of E50 (Figure 1). Mitoses were observed in the neuroepithelium at E50 and E80 (Figure 2 A and B). Apoptosis characterized by nuclear fragmentation, pyknosis, and phagocytosis of the apoptotic body by macrophages was observed mainly in proliferative zone at E80 (Figure 2 C through E).

By immunohistochemistry at E50 and E80, PCNA-positive cells were detected mainly in proliferative zone (Figure 3 A and B). PCNA-positive cell counts were 771.5 and 618 per 1000 cells at E50 and E80, respectively. However, few PCNA-positive cells were found in intermediate zone and cortical plate (Table 1). GFAP immunoreactivity was detected in the neuroepithelium of the proliferative zone (Figure 3 C and D). Radial glial fibers elongating vertically from the proliferative zone to cortical plate were strongly positive (Figure 3 E). Iba1 immunoreactivity was detected in all layers, particularly at E80, when many positive cells were localized in proliferative zone (Figure 3 F). In addition, some positive cells phagocytized cellular debris (Figure 2 F). NeuN immunoreactivity was not detected at either E50 or E80 (data not shown).

TUNEL-positive cells at E50 and E80 were sparsely distributed in each layer (Figure 2 G), except for the cortical plate at E50, when positive cells were not detected. Overall there were very few TUNEL-positive cells (0.6 to 2.1 per 1000 cells; Table 1). Caspase 3 immunoreactivity was not detected.

Differentiation of neural cells at E120 and E150. Histologically, the cerebral cortex at E120 and E150 consisted of 6 layers (Figure 4 A and B). No cells at either time point showed characteristics of apoptosis.

Immunohistochemically, PCNA-positive cells were detected mainly in the ventricular zone, with a few PCNA-positive cells in the white matter and cerebral cortex at E120 and E150. PCNA-positive cell counts in ventricular zone were 833.1 and 658.3 per 1000 cells at E120 and E150, respectively (Table 2). NeuN immunoreactivity was detected in layers III through VI at E120 and in all layers at E150 (Figure 4 C and D; Table 3). Moreover, NeuN-positive cells at E120 had scant cytoplasm (Figure 4 C

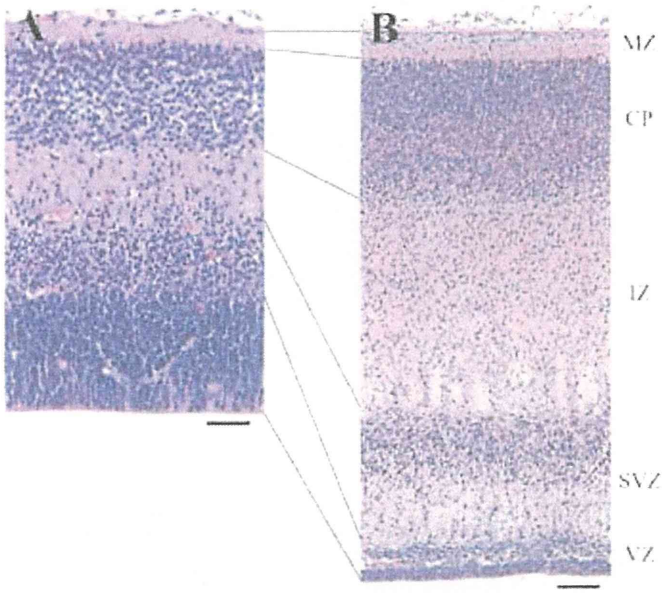

Figure 1. Cerebral wall at (A) E50 and (B) E80. The cerebral wall consisted of the marginal zone (MZ), cortical plate (CP), intermediate zone (IZ), subventricular zone (SVZ), and ventricular zone (VZ). Hematoxylin and eosin stain; bar, 50 μm.

inset), whereas at E150, some cells had abundant cytoplasm with processes resembling those of mature neurons (Figure 4 D inset). Radial glial fibers that were positive for GFAP were not present (Figure 4 E), the white matter contained many GFAP-positive cells with multiple processes (Figure 4 F) at E120 and E150. Iba1 immunoreactivity was present in each layer at E120 and E150. There were no TUNEL- or caspase 3-positive cells in any section at E120 or E150.

Discussion

This study investigated the proliferation, differentiation, and distribution of apoptosis of neural cells and the involvement of microglia in removal of apoptotic cells in the fetal cynomolgus monkey brain, especially the cerebral cortex, at different developmental stages. Because few studies have addressed the precise neural development of the cynomolgus monkey fetal brain, we mainly compared our results with those in rodents, humans, and rhesus monkeys (*Macaca mulatta*).

Proliferation and the migration of neural cells are known to be important in CNS development.[5] In our study, we noted a high frequency of mitoses in the ventricular zone at both E50 and E80. Using immunohistochemistry with PCNA to detect the proliferative activity of neural cells, we noted many positively stained cells in the proliferative and ventricular zones from E50 to E150. This finding of many mitotic cells in the ventricular zone is consistent with previous reports.[22,32] Moreover, the production of cortical neurons in the monkey visual area has been reported to start at E40 and finishes by E100.[25] Therefore, we speculate that cortical neurons actively proliferate between E50 and E80 and that this division and proliferation is complete by E120. Other reports show that numbers of PCNA-positive cells are significantly reduced when cell migration is active,[22,32] and these cited results are inconsistent with our finding that proliferative activity

Table 1. Number of PCNA- and TUNEL-positive cells per 1000 cells in each layer of the cerebral wall at E50 and E80

	E50		E80	
	PCNA	TUNEL	PCNA	TUNEL
Cortical plate	0	0	0.2	0.7
Intermediate zone	0.2	0.6	0.6	1.6
Proliferative zone	771.5	1.2	618	2.1

Table 2. Number of PCNA- and TUNEL-positive cells per 1000 cells in each layer of the cerebrum at E120 and E150

	E120		E150	
	PCNA	TUNEL	PCNA	TUNEL
Layers I through VI	10.4	0	10.3	0
White matter	77.9	0	42.5	0
Ventricular zone	833.1	0	658.3	0

Table 3. Number of NeuN-positive cells per 1000 cells in each layer of the cerebral cortex at E120 and E150

Layer	E120	E150
I-II	25.1	894.7
III	674.3	946.5
IV	673.6	947.7
V	557.2	929.5
VI	681.4	952.4

NeuN-positive cells were not detected at E50 and E80.

in the ventricular zone is maintained at a high level after E120. Whereas the previous studies addressed the human fetal brain,[22,32] we used the cynomolgus monkey fetus, and differences observed may reflect species-associated differences between humans and macaques in neural cell development during the final stage of CNS maturation.

We noted few PCNA-positive cells in the intermediate zone and cortical plate at E50 and E80. PCNA-positive cells increased in the cerebral cortex and medulla at E120 and E150, but frequencies were lower than those in the ventricular zone. Humans display a few PCNA-positive cells in intermediate zone.[22,32] In addition, the presence of PCNA-positive cells in the intermediate zone has suggested their role in the glial system.[17] In the rat developing brain, most microglial precursors show high proliferative activity,[8] and the proliferating cells in the cortical plate are thought to be glioblasts or angioblasts.[5] In light of these previous and our current findings, we speculate that PCNA-positive cells at E50 and E80 in areas other than the proliferative zone might be glial cells.

Apoptosis plays an important role in the developing CNS.[5,7] In human cerebral development, apoptosis is induced mainly in the proliferative zone during early pregnancy (11 gestational weeks [GW]),[26] increases in all regions of the telencephalon and from marginal zone to ventricular zone except for cortical plate during the second trimester of pregnancy,[26,31] and is detected in the cerebral cortex during late pregnancy.[26,33] In proliferative zone at E80 in the present study, we observed chromatin condensation and nuclear fragmentation, which are well-known morphologic characteristics of apoptosis. We noted only a few TUNEL-positive cells in each layer at E50 and E80 and no TUNEL-positive cells at all after E120. Moreover, there was little difference in temporal